

# Perspectives and Emerging Trends in Plasma Catalysis: Facing the Challenge of Chemical Production Electrification

Annemie Bogaerts,<sup>[a]</sup> Gabriele Centi,<sup>\*[b]</sup> Volker Hessel,<sup>[c, d]</sup> and Evgeny Rebrov<sup>[d, e]</sup>

Electrification of chemical production requires the development of innovative solutions, with plasma catalysis being among them. This perspective summarizes many years of studies and discussions made in the frame of the ERC Synergy project SCOPE dedicated to the above aspects. However, it does not aim to overview the project results but rather use them in combina-

tion with literature indications to outline the emerging trends and present gaps to pass from a research area to a key technology to develop sustainable production and associated changes required in the modalities of production. The perspective thus aims to offer a vision of the future for plasma catalysis and its role in facing societal challenges.

## 1. Introduction

Electrification of chemical production, e.g., the use of renewable energy sources (RES) to reduce the use of fossil fuels and carbon footprint, is undoubtedly a main driver for innovation, which will induce a radical redefinition of the technologies and processes for chemicals and fuel production.<sup>[1]</sup> This ongoing transformation also has a significant impact on catalysis. There is a clear shift of research interest from traditional “thermal” catalysis (for refinery, petrochemistry, and biomass transformation) to technologies using RES directly or using the electricity produced from them.

The term “thermal” is used here to indicate conventional heterogeneous catalysis, where the energy to overcome the activation energy is provided by heat (e.g., all solid catalysts have a threshold temperature to be active). However, technologies such as photo-, electro-, and plasma catalysis operate (typically) at temperatures below this threshold. The energy is provided by the generation of “hot” species, like charges induced by light absorption in semiconductors (photo), the generation of surface charges by applying an electrical potential (electro), or

the generation of “hot” electrons and their reaction with gas molecules, generating radicals, or excited or charged molecules, which interact with the catalyst, the latter effect also generating charges on the catalyst (nonthermal plasma (NTP)). There are thus common aspects in these technologies, with marked differences to “thermal” catalysis. For this reason, we have called them with the concise indication of “reactive” catalysis trio.<sup>[2]</sup>

Note that the term electrification is also used to indicate a current trend in chemical reactors where the heat is produced electrically, directly (electrical heaters), or by inducing the catalyst heating via the Joule effect or other mechanisms.<sup>[3]</sup> However, in these cases, it only changes the mechanism of heating (with an influence on thermal gradients, heat transfer, etc.). Still, the intrinsic catalytic mechanism is not changed. Similar are the cases of solar heating or heating induced by microwaves. Instead, we use the term electrification in the strict concept of technologies where “reactive” species (charges, radicals, etc.) are produced, typically at room temperature, by light absorption, application of potential, or interaction with species generated by NTP. These “reactive” catalysis technologies operate (typically) at room temperature using RES and are also characterized by a rapid switch on/off, a property crucial in exploiting RES. Furthermore, they are well-suited for distributed applications, another emerging trend.<sup>[4]</sup>

Due to the different intrinsic features of reactive versus thermal catalysis, the impressive body of knowledge developed for the latter can only be partly translated into reactive catalysts. Notwithstanding the impressive number of studies on the latter, effective progress is still limited. There is an increasing gap between expectations (also fixed in political targets) and effective progress in facing the challenges associated with the occurring transformation of our society to a new low-carbon and resilient (sustainable) model.

It is necessary to accelerate the innovation process. We commented earlier that rather than continuing (only) the current scientific approach, there is a need for a broader vision that explores unconventional directions and catalysis to widen the current horizons.<sup>[5]</sup>

We focus this perspective on plasma catalysis, highlighting how this “unconventional” catalysis offers many clues to address

[a] A. Bogaerts  
Research group PLASMANT, Department of Chemistry, University of Antwerp, Wilrijk, Antwerp BE-2610, Belgium

[b] G. Centi  
Department ChiBioFarAm, University of Messina, ERIC aisbl and CASPE/INSTM, Messina 98166, Italy  
E-mail: centi@unime.it

[c] V. Hessel  
School of Chemical Engineering and Advanced Materials, The University of Adelaide, Adelaide SA 5005, Australia

[d] V. Hessel, E. Rebrov  
School of Engineering, University of Warwick, Library Rd, Coventry CV4 7AL, UK

[e] E. Rebrov  
Department of Chemical Engineering and Chemistry, Eindhoven University of Technology, P.O. Box 513, Eindhoven 5600 MB, The Netherlands

© 2025 The Author(s). ChemCatChem published by Wiley-VCH GmbH. This is an open access article under the terms of the [Creative Commons Attribution License](#), which permits use, distribution and reproduction in any medium, provided the original work is properly cited.

the complex challenges outlined above. However, a step forward in understanding the possibilities it offers is necessary. Indeed, plasma catalysis is clearly different from thermal catalysis, as explained above and in the next sections. This perspective offers clues to use creative and original solutions beyond the current trends, defining prospects, emerging trends, and gaps to overcome. Note that we focus here on nonthermal plasma (NTP), which is clearly different from thermal plasmas.<sup>[6]</sup> Indeed, in thermal plasmas, the temperature (or energy) of all plasma species, including gas molecules, ions, excited species, and electrons, is equal to each other. Typically, it is in the order of 10,000 K. This is clearly too high for catalyst implementation inside the plasma (so-called in-plasma catalysis). However, catalysts can still be placed postplasma and activated by the hot gas leaving the plasma reactor. In contrast, NTP is characterized by a much higher electron temperature (order of several eV, or several 10,000 K) than the gas temperature (room temperature or slightly above), and this allows electron-impact ionization, excitation, and dissociation of the gas molecules, creating ions, excited molecules, and radicals, which can interact directly with a catalyst surface, as the latter can be directly implemented inside the plasma reactor, due to the low gas temperature.

It is worth mentioning that electron-impact reactions also activate the molecules without a catalyst, thus creating a highly reactive mix of radicals, excited species, and ions, which can easily form new molecules. However, this high chemical reactivity means that plasma cannot selectively produce targeted products, and by combining plasma with catalysts, we aim to produce value-added compounds, such as oxygenates, selectively.

The main aim of the combination of NTP plasma and catalysis is the use of the latter to drive the reaction along the aimed path selectively or, sometimes, to inhibit back reactions, often limiting the performances. However, usually, the activated species generated in NTP plasma (radicals, vibrationally excited species, etc.) are quenched (i.e., inactivated) by the interaction with the solid catalyst. Thus, in essence, the question of plasma catalysis is to find a way in which there is an effective synergy between the two by properly designing the catalysts to interact positively with the species generated in the NTP plasma.<sup>[7]</sup> Many of the often contrasting literature results depend on the still scarce effort to understand how to realize this synergy. It should be remembered that there are also other indirect effects of NTP plasma induced on the catalyst, such as its thermal heating or charging of the surface, as well as inducing metastable reconstructions of the catalyst surface.<sup>[8]</sup> A solid, as discussed later, can also physically change the characteristics of the plasma discharges, thus altering the features themselves of the plasma. Thus, in the discussion of synergies between plasma and catalysis, it is necessary to clarify when these side effects are not present.

This perspective summarizes the six years of studies and discussions made in the frame of the ERC Synergy project SCOPE dedicated to the above aspects. It involves the four principal investigators working on this project in different locations. However, the aim is not to overview the results but to put them in the perspective of the state-of-the-art, especially the emerging trends. The perspective thus aims to offer a vision

of the future for plasma catalysis and its role in facing societal challenges.

## 2. Emerging Possibilities in Modeling

While plasma catalysis is gaining increasing interest for various applications (e.g., Ref. [9]), the underlying mechanisms are very complex because the plasma affects the catalyst, and the catalyst (or packing material) affects the plasma behavior in many ways.<sup>[8c,10]</sup> In addition to the aspects commented above, the plasma may cause changes in the physicochemical properties of the catalyst (e.g., higher adsorption probability, higher surface area, a change in the oxidation state, reduced coke formation, thus preventing deactivation of the catalyst, and a change in the work function), thus affecting the catalytic activity.<sup>[11]</sup> In addition, plasma may also lead to hot spot formation, possibly modifying the local plasma chemistry,<sup>[12]</sup> and it can reduce the activation barriers and induce changes in the reaction pathways because of the presence of reactive plasma species.<sup>[13]</sup> Vice versa, the catalyst may enhance the local electric field strength in the plasma,<sup>[14]</sup> yielding a rise in the high energy tail of the electron energy distribution. It can also change the discharge type from streamers inside the plasma to streamers along the catalyst surface, which might result in more intense plasma around the contact points, thus affecting the plasma chemistry.<sup>[15]</sup>

Thus, more insight is needed to design optimal catalysts tailored to the plasma environment and vice versa, to tune the plasma conditions and plasma reactor design to work in optimal synergy with the catalyst. It has become increasingly clear from recent experiments that catalysts often modify the plasma electrical behavior rather than act as real chemical catalysts (e.g., Refs. [15a, 16]). These effects must be better understood, but it is often not reported data that can understand whether these effects are present and what their impact is. Hence, in the following sections, we will discuss in more detail the need for a better understanding and how modeling can contribute to this for these three aspects, i.e., (1) tuning catalyst material and plasma conditions to each other for better synergy, (2) improved plasma reactor design for optimal plasma–catalyst interaction, and (3) the effect of catalysts on the plasma electrical behavior.

### 2.1. Tuning Catalyst Material and Plasma Conditions to Exploit Plasma–Catalyst Synergy

Plasma catalysis research is often still based on trial and error, coupling with a thermal catalyst because it is active in similar reactions. However, there is a clear difference between thermal and plasma catalysis, as outlined in the Introduction (note that we refer here to conditions where the plasma does not act simply in heating the solid catalyst). In NTP plasma catalysis, the plasma already activates the reactant molecules, producing many reactive species, like radicals, electronically and vibrationally excited species, ions, and electrons, which can all react at the catalyst surface. Hence, the catalyst should optimally interact with these reactive species without simply

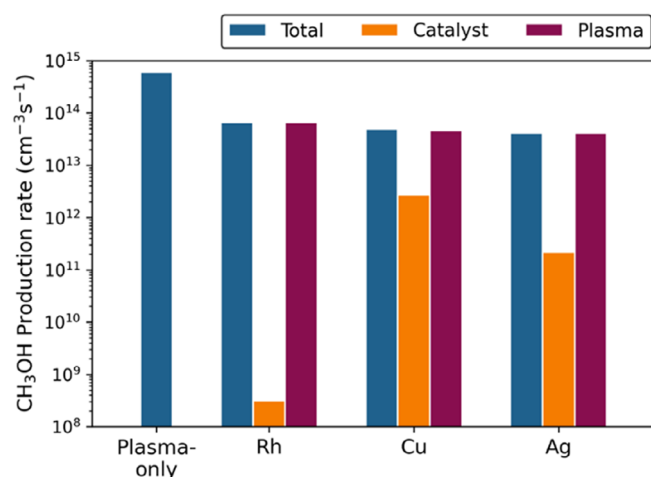


**Figure 1.** CH<sub>3</sub>OH production rate, calculated by the model of Loenders et al.,<sup>[8d]</sup> for plasma without catalyst and combined with Rh, Cu or Ag catalysts for DRM from a 1:1 CO<sub>2</sub>/CH<sub>4</sub> mixture. Plotted are the total reaction rate, the rate on the catalyst surface, and inside the plasma (see legend). Note that the rates are logarithmically scaled; hence, the production rates at the catalyst surface are several orders of magnitude smaller. The model predicts that the CH<sub>3</sub>OH production rate in plasma-only is higher than in combination with these metal catalysts because the catalysts scavenge the plasma-produced radicals (see text). Note that this model considers pure metals (plane surface) and does not account for certain metal loading, or metal-support interactions, surface defects, different facets, or transport of species to and from the catalyst surface. See the reference for further details. Adopted from Loenders et al.,<sup>[8d]</sup> with permission.

quenching them. Indeed, recent modeling for dry reforming of methane (DRM) predicted that the plasma-produced radicals are quenched at a metal catalyst surface and rather recombine back into the reactants than react further into the desired products.<sup>[8d]</sup>

Moreover, as a result of this quenching, the radical concentration in the plasma drops, leading to lower reaction rates in the plasma phase, and thus, the overall rate of producing value-added chemicals can be lower in plasma catalysis than in pure plasma without catalysts (see Figure 1). While this result is based on chemical kinetics model predictions (without accounting for transport to and from the catalyst surface, which may affect the outcome), similar behavior is also often observed in experiments (e.g., Ref. [17]). In other words, the catalyst seems to act more as an “anti-catalyst” by quenching the plasma-produced radicals.

Hence, these modeling insights reveal that metal catalysts should be combined with promoting other reactive species in the plasma rather than radicals, such as vibrationally or electronically excited molecules, because they would reduce the dissociation energy barrier at the catalyst surface, thus enhancing the catalytic reactions.

However, the most common plasma type for plasma catalysis, i.e., a dielectric barrier discharge (DBD), produces more radicals than excited species because it operates at quite high reduced electric fields, generating electrons with quite high energy (at least several eV). Note that the reduced electric field stands for the ratio of the electric field over gas number density. It is commonly used to characterize plasma, specifically the importance of certain electron impact reactions, as they are determined

by the electron energies that follow from the reduced electric field. Therefore, the plasma conditions should be tuned (specifically the reduced electric field and, thus, the electron energy) to selectively produce vibrationally or electronically excited species, as the latter can give rise to more plasma–catalyst synergy. We believe modeling can help to find such optimal plasma conditions.

For this purpose, more-dimensional, fully coupled computational fluid dynamics (CFD) models are needed, which solve all relevant plasma physics, including gas flow dynamics, heating, and electrical behavior, besides the chemistry, and also account for the transport of species toward and from the catalyst surface. Some 2D axisymmetric models have already been developed for packed bed DBD reactors used in plasma catalysis (e.g., Ref. [18]), albeit without accounting for gas flow dynamics and heating. Clearly, extending such models would be needed to predict which plasma operating conditions and/or reactor designs could lead to more suitable reduced electric fields for producing vibrationally and electronically excited levels, thus promoting plasma-catalysis synergy.

However, developing such models will require major efforts because of the complex interplay between physics and chemistry. Nevertheless, such fully coupled models have now become feasible, as they were recently developed for other plasma reactors.<sup>[19]</sup> Hence, if such models could predict how vibrationally and electronically excited levels can be maximized in typical plasma catalysis reactors and, thus, how plasma–catalyst synergy could be optimized, they could cause a paradigm shift in plasma catalysis.

The other option, next to tuning the plasma conditions for optimal synergy with the catalysts, is to design catalysts perfectly tailored to the plasma conditions, and modeling can also help obtain more insights.

One way to find the optimal catalysts would be by catalyst screening, ideally in combination with machine learning (ML). There are some recent examples in which ML could reveal the relative importance of various plasma process parameters for the reaction performance, either in catalyst-free DRM to higher value oxygenates,<sup>[20]</sup> and also for Ni/Al<sub>2</sub>O<sub>3</sub> catalysts.<sup>[21]</sup> In contrast to microkinetic models for plasma–catalyst interactions (such as Ref. [8d] and described below), which typically consider simple bulk metals, ML could be applied to more complex catalysts, as they are based on experimental data so that they can account for the effects of promoters and catalyst-support interactions.

Nevertheless, ML is less suited to elucidate the underlying mechanisms, and the potential of ML in plasma catalysis is also still limited due to the requirement of a very large experimental data set, which is often still a problem in plasma catalysis. Hence, systematic catalyst screening is needed for a large number of catalysts (50 or more, all for the same reaction and conditions) to provide sufficient data for ML and guide the design of the most suitable catalysts for plasma catalysis.

On the other hand, a thorough understanding of plasma-catalytic mechanisms will also help design better catalysts. Here, modeling can be of great value, preferably in combination with in situ surface characterization. The latter was explained in more detail in our previous paper,<sup>[5a]</sup> so here we will focus on the

needs and potential of detailed surface microkinetic models for plasma catalysis.

There are already several plasma catalysis surface microkinetic models for various reactions, such as nonoxidative coupling<sup>[22]</sup> and oxidative coupling of CH<sub>4</sub>,<sup>[23]</sup> CO<sub>2</sub> hydrogenation,<sup>[24]</sup> and NH<sub>3</sub> synthesis.<sup>[25]</sup> For instance, the model of Engelmann et al.<sup>[25c]</sup> was applied to a wide variety of catalyst materials and predicted that when radical adsorption and Eley-Rideal (ER) reactions determine the reaction pathways, the NH<sub>3</sub> synthesis was quasi-independent of the catalyst material, resulting in rather flat volcano plots, in agreement with various experimental data (e.g., Refs. [15a, 26]). This confirms that in most common (DBD) plasma-catalytic conditions, radical adsorption and ER reactions might indeed dictate the plasma-catalytic NH<sub>3</sub> synthesis mechanisms. This is in line with the model predictions of Loenders et al.<sup>[8d]</sup> for the dominant role of radicals in plasma-catalytic DRM, discussed above.

The model predictions of Loenders et al.<sup>[8d]</sup> and Engelmann et al.<sup>[25c]</sup> are nice examples of how modeling can help to gain more insight into the underlying plasma-catalyst interactions. Still, they show the limitation of plasma catalysis and why plasma-catalyst synergy is often not very pronounced in experiments. Indeed, we attribute this to the dominant role of plasma radicals and thus the fact that the plasma reactivity is already very high without catalysts. At the same time, metal catalysts scavenge the radicals, lowering their concentration in the plasma, and thus the rates of plasma reactions. This fact again stresses the need to search for other catalysts that do not scavenge the radicals, or vice versa, to tune the plasma conditions for exploiting vibrationally and electronically excited species rather than the radicals, as discussed in the next section.

In general, such chemical kinetic models can elucidate how various plasma species affect the catalyst surface chemistry in order to support experiments in tuning the plasma conditions to maximize the desired reactive species. However, they cannot yet predict which catalysts would be more suitable to work in optimal synergy with the plasma species. The reason is that such models need input data, such as reaction and activation enthalpy and entropy (in order to calculate rate coefficients), typically from density functional theory (DFT), which is not available for a wide variety of catalyst materials. Typically, it is available for bulk metal catalysts, explaining why the above models all apply to metal catalysts indeed. Still, data for other materials, such as metal oxides, are much more scarce. Hence, there is a clear need for more DFT studies on other catalyst materials to be used as input in plasma catalysis microkinetic models.

In addition, there is a crucial need for more sophisticated models that describe not only the catalyst surface chemistry but also the fully coupled plasma and surface chemical kinetics and thus provide information on how the catalyst affects the plasma species concentrations. The model of Loenders et al.<sup>[8d]</sup> is such a fully coupled model and indeed yields very valuable information, such as the quenching of radicals at the catalyst surface, resulting in lower radical concentrations in the plasma and, thus, overall, a lower reactivity (cf. Figure 1 above). However, it is limited to bulk metal catalysts. It cannot yet account

for other catalyst materials (due to too limited DFT input data, as discussed before). It also does not take into account the transport of species to and from the catalyst surface, as well as the microscopic structure of catalyst materials or metal-support interactions, which may affect the findings. Hence, there is a need to develop more sophisticated models that include such effects as well.

Finally, other plasma components, such as the electric field and surface charging, may also play a role in plasma catalysis, as they can modify the electronic structure of the material. Still, these effects are typically not included in the above surface chemical kinetics models. Bal et al.<sup>[27]</sup> and Jafarzadeh et al.<sup>[28]</sup> studied these effects by DFT simulations. The model of Bal et al.<sup>[27]</sup> revealed that charging a dielectric Al<sub>2</sub>O<sub>3</sub> surface loaded with a single metal atom (Ti, Ni, or Cu) affects its chemical reactivity. Specifically, surface charging was found to activate the CO<sub>2</sub> molecule upon adsorption. Likewise, Jafarzadeh et al.<sup>[28a]</sup> predicted that the adsorption energies of CO<sub>2</sub> on TiO<sub>2</sub>-supported Ni<sub>5</sub> and Cu<sub>5</sub> catalyst clusters substantially rise upon charging. Finally, Jafarzadeh et al.<sup>[28b]</sup> also developed a plasma catalysis model, accounting for the effect of both charging and electric fields on the adsorption and activation of CO<sub>2</sub> on various Cu surfaces. Recently, DFT modeling was also applied by Kim et al.<sup>[29]</sup> to study the role of plasma-induced charging and electric fields, showing that plasma reduces the effective binding energy of CO on the Pt surface. However, more insights, both from modeling and experiments, are still needed to understand better how these (and other) plasma components can affect the catalyst during operation, both structurally and compositionally.

## 2.2. The Need to Improve Plasma-Catalyst Contact for Optimal Plasma-Catalyst Interaction

Another (and perhaps the most crucial) limitation in plasma catalysis setups that must be overcome is the limited contact between plasma and catalyst. Indeed, the reactive plasma species have a short lifetime and often do not reach the catalyst surface, so the chemical reactions inside the plasma are dominant. We believe this might also be the reason why no beneficial effect is often observed in plasma catalysis versus pure plasma studies (e.g., Ref. [17]). Hence, more insights are needed to design plasma reactors with guaranteed transport of plasma species to the catalyst surface.

The most common catalytic packing is based on beads in a packed bed, on which the catalyst is “coated” (e.g., Refs. [15a, 16]), although pellets can also be used. Typical bead sizes are in the order of 1–2 mm diameter, but reducing the bead size could be beneficial, as it would also reduce the void size in the packed bed and thus enhance contact between plasma and the catalyst surface. Wang et al.<sup>[30]</sup> experimentally investigated plasma-catalytic DRM using smaller beads (i.e., 120–2390 nm diameter). They found optimal performance for the beads with a 740 nm diameter, showing clear enhancement compared to an empty reactor (pure plasma conversion). Hence, this is an important insight for improving plasma-catalyst contact. However, care must be taken that there is not too much pressure

build-up in the packed bed, and the void sizes must also be large enough for plasma streamers to propagate.

Van Laer et al.<sup>[18b]</sup> developed a CFD model to study the effect of bead size (although not yet in the sub-mm range) on the electrical plasma characteristics (e.g., electric field, electron density, and temperature). However, for the sake of computation time, this model was developed in helium with limited chemistry. Moreover, the use of helium gas made it possible to assume a uniform plasma, and hence, no streamer propagation was investigated. Wang et al.<sup>[18d]</sup> developed a CFD model in air, describing streamer propagation and nicely showing the effect of the dielectric constant of the beads, changing the plasma behavior from surface ionization waves at low dielectric constant to localized filamentary discharges at high dielectric constant, also validated by experiments. However, this model did not investigate the effect of bead size. Moreover, it was also not fully coupled with the gas flow dynamics, to investigate e.g., pressure build-up. Nevertheless, extending this model could provide valuable information on how to optimize the catalyst packing for enhanced contact between reactive plasma species (preferably excited species) and the catalyst surface.

In addition, plasma streamer propagation through a packed catalyst bed was also studied by particle-in-cell–Monte Carlo collision (PIC–MCC) simulations,<sup>[31]</sup> as well as for other catalyst support shapes, such as honeycombs or three-dimensional fiber-deposition (3DFD) structures.<sup>[32]</sup> The latter could, in principle, also enhance contact between plasma and catalyst. However, PIC–MCC simulations are very time-consuming, and hence, they include only limited chemistry. Moreover, they are less suitable for coupling to the modeling of gas flow dynamics. We believe fully coupled CFD models will be needed to investigate which catalyst packing or support shapes can enhance the contact between plasma species and the catalyst surface.

Finally, another way to enhance the contact between plasma and catalyst surface is by designing catalyst supports with large enough pore sizes so that the plasma streamers can penetrate the pores, which greatly increases the catalyst surface area in contact with the plasma. Computer modeling, based on either the CFD approach (for helium plasma)<sup>[14a,33]</sup> or PIC–MCC simulations (for air plasma)<sup>[34]</sup> already revealed that the so-called Debye length defines the minimum pore size needed for plasma penetration. The latter is typically at least 600 nm at typical plasma catalysis (DBD) conditions, depending on electron density and temperature in the plasma streamer.<sup>[34]</sup> However, most catalytic supports (e.g., zeolites) have much smaller pores (nm range), and thus, plasma streamers cannot penetrate inside these pores. Hence, catalyst nanoparticles deposited inside the pores of such supports would not be reached by the plasma streamers. Nevertheless, when the pores are too small for plasma streamer penetration, it might still be possible for plasma species to diffuse into the pores. However, because of their short lifetime, these species might also not reach deep inside the pores. Again, modeling can help to obtain more insight into how the catalytic supports and plasma reactor design/conditions can be tuned to each other for optimum plasma–catalyst interaction.

On the other hand, small catalyst pores can also be beneficial for the so-called “shielding protection” of products like  $\text{NH}_3$ , which can diffuse into the pores, thereby shielding them from the plasma and protecting them from plasma-induced decomposition. This was illustrated by Rouwenhorst et al.<sup>[35]</sup> for zeolite 4A. Desorption after plasma is turned off resulted in much higher  $\text{NH}_3$  yields, i.e., a factor of two compared to without using an adsorbent. Wang et al.<sup>[36]</sup> reported a similar effect for mesoporous MCM-41, although thermal desorption of  $\text{NH}_3$  was not considered here.

### 2.3. Effect of Catalysts on the Plasma Electrical Behavior

The above issue, e.g., that catalyst nanoparticles deposited inside the pores might not be reached by the plasma streamers (or even not by diffusion of reactive plasma species), can be overcome using a catalyst synthesis method that only deposits catalyst particles at the outside surface of the beads so that they will all be in contact with the plasma.

For this purpose, De Meyer et al.<sup>[16]</sup> compared two catalyst synthesis methods, i.e., wet impregnation (where the catalyst nanoparticles are more or less uniformly distributed over the beads, hence also inside the pores) and spray coating (where the catalyst nanoparticles are deposited at the outer surface of the beads, resulting in a quite uniform metallic coating on the dielectric beads). The authors observed significant differences in the catalytic performance, both for DRM and  $\text{NH}_3$  synthesis, which they could attribute to differences in the plasma electrical behavior. Indeed, while the bare  $\text{Al}_2\text{O}_3$  dielectric beads and some of the wet impregnation catalysts gave rise to a clear filamentary discharge, the spray-coated catalysts resulted in a quite uniform plasma, with very few (and weak) microdischarge filaments. A similar effect was also reported by Ndayirinde et al.,<sup>[15a]</sup> who correlated variations in  $\text{NH}_3$  production with changes in the plasma electrical characteristics. They concluded that the catalysts had limited surface chemical-catalytic effects but could be seen as “plasma modifiers.” We believe this aspect is still largely underestimated in plasma catalysis research, while it is very important. Hence, when searching for optimal catalysts, more attention should also be paid to how the catalyst material affects the plasma electrical behavior, besides their chemical-catalytic behavior.

The change in plasma electrical behavior obviously also affects the plasma-catalytic performance, which was observed to be different for DRM versus  $\text{NH}_3$  synthesis. Indeed, for DRM, the filamentary behavior appeared somewhat beneficial, while for  $\text{NH}_3$  synthesis, the results were much better in the uniform plasma.<sup>[16]</sup> Both these observations are in line with earlier 0D chemical kinetics computer model predictions. Indeed, for DRM, Snoeckx et al.<sup>[37]</sup> showed that the  $\text{CO}_2$  and  $\text{CH}_4$  molecules are mainly dissociated during the microdischarge filaments. In contrast, for  $\text{NH}_3$  synthesis, van 't Veer et al.<sup>[38]</sup> predicted that the  $\text{NH}_3$  molecules are destroyed during the microdischarge filaments, and there is net formation in the afterglows in between the filaments. Hence, a more uniform plasma with fewer and

weaker filaments is beneficial for  $\text{NH}_3$  synthesis, which is in line with the experiments of De Meyer et al.<sup>[16]</sup> This is a clear example of how modeling can help to understand experimental observations.

However, the above models were 0D chemical kinetics models, hence focusing on detailed chemistry, without a self-consistent description of microdischarge filament formation, i.e., the microdischarges were input in the model as pulses of higher plasma power.<sup>[37,38]</sup> To describe the entire picture, including not only the chemistry but also the plasma physics, more-dimensional fully coupled CFD models, describing the gas flow dynamics, plasma electrical behavior, plasma chemistry, and species transport, must be developed. In principle, these models should be developed in 3D to fully account for the packed bed geometry, which does not exhibit 2D axisymmetry.

In the past, the 3D geometry was mimicked by two complementary 2D axisymmetric models, accounting either for (i) the physical contact between the beads or (ii) the void space in between the beads, which is indeed present in a 3D packing and allows plasma (streamers) to penetrate.<sup>[18c]</sup> However, that model was developed in helium, characterized by a uniform plasma, and hence, it did not explicitly describe streamer propagation. Indeed, at the time of developing that model, this would have led to excessive calculation times. However, as computers become faster, such a fully coupled 3D (or 2D axisymmetric) modeling approach might now be feasible, even in reactive gases, which are more interesting for plasma catalysis applications and where streamer propagation definitely must be accounted for. Finally, the ultimate models should also integrate chemical reactions at the catalyst surface to obtain the entire picture. This will allow us to investigate whether catalysts act mainly as plasma modifiers or how they can also be fully exploited as chemical catalysts.

In summary, there is a clear need for fully coupled plasma catalysis models that integrate plasma and surface chemical kinetics models, like,<sup>[8d]</sup> but also describe the gas flow dynamics, plasma electrical behavior (such as streamer propagation), and species transport inside the plasma, and also toward and from the catalyst surface.

The ultimate multi-scale plasma catalysis model could be represented by Figure 2, describing the coupled and detailed plasma and surface chemistry (with 0D modeling, for the sake of computation time), using input from atomic-scale (DFT) simulations, in combination with 2D/3D fluid dynamics modeling of the macroscopic plasma behavior (including gas flow and heating, plasma electrical behavior, species transport, and chemistry), as well as the microscopic picture of plasma streamer penetration inside the pores of catalytic support materials.

### 3. New Trends in Reactor, Electrode, and Catalyst Design

Differently from the thermal catalysis case, where the catalyst and reactor design are often treated separately (even if their design should be integrated), in plasma catalysis, there is a greater need for a coupled integrated approach.<sup>[32,39]</sup> Different

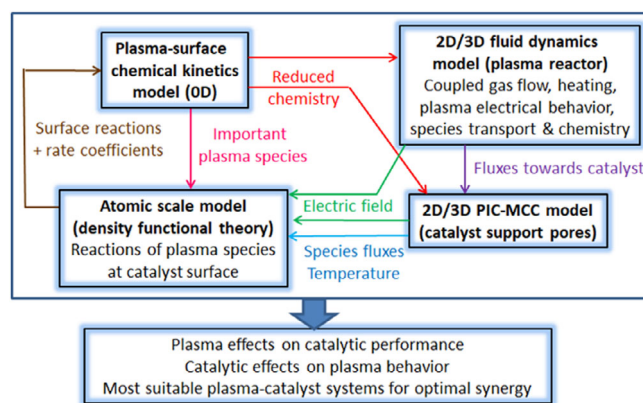


**Figure 2.** Scheme of the ultimate multi-scale plasma catalysis model, based on detailed plasma and surface chemistry (0D) modeling, using input from atomic-scale (DFT) simulations, and combined with 2D/3D fluid dynamics modeling of the macroscopic plasma behavior and PIC-MCC simulations of the microscopic picture of plasma streamer penetration inside the pores of catalytic support materials.

reactor types require different catalysts with reduced catalyst loadings or no catalyst at all. Electrode design should be part of the reactor design, and catalysts may often be deposited on the electrodes, changing their characteristics. The approach from classical reactors cannot be applied to plasma reactors. In addition, the catalyst may often also act as an electrode. An integrated approach is thus required to reach the synergy. The plasma influences the catalyst, and vice versa, as commented before.

It must be mentioned, however, that a better logical approach would be to discuss specific objectives, i.e., how to:

- maximize the formation of excited species (including by field change);
- ensure these excited species reach the catalyst (interface);
- prevent “anti-effects” (anti-catalysis, as commented before).

There is clearly a high interrelation between the catalyst, electrode, and plasma reactor design to reach the above objectives. Thus, the reactor, electrode, and catalysts are complementary aspects to reach the same objectives. It is not correct to separate them, but this introduces a further factor of complexity to the already complex plasma catalysis topic. Therefore, to help readers follow the rationale, we separate the discussion and catalysts and reactor/electrode design below because this is the common approach reported often in the literature.

#### 3.1. Catalysts Design in Relation to Plasma Reactor

In order to perform plasma-assisted catalytic reactions most efficiently, the plasma species formed inside the plasma discharges should reach the catalyst surface faster than they would react via nonselective pathways in the discharge volume. However, as also discussed in the previous section, most plasma species are short-lived with a characteristic lifetime in the order of hundreds of microseconds to milliseconds. Their slow diffusion in micro- and mesoporous supports results in most of the plasma species only reaching the outer surface of the support, or they even

react in the discharge volume, not reaching the catalyst surface at all.<sup>[40]</sup> Still, the catalyst can change the electric field intensity in the space between the catalyst particles, thus acting as “plasma modifiers,” as discussed above. However, this is rather a physical effect, and it is mainly associated with the ferroelectric properties of the support material.

In some studies, the catalytically inactive supports showed even better conversion performance than the supports loaded with active metals due to the physical influence on the discharge.<sup>[17b,d]</sup> It is also possible that ferromagnetic materials (with a high dielectric constant such as BaTiO<sub>3</sub>)<sup>[8c]</sup> change the plasma discharge mode in DBD reactors from filamentary to a surface-confined discharge,<sup>[41]</sup> so the plasma is formed only in a narrow layer near the surface of the particles rather than homogeneously in the entire reactor volume.

Typically, this has a negative effect on the conversion in the case of wall-coated DBD reactors. It should be mentioned that the catalyst bed also reduces the available discharge volume and, consequently, the residence time of reactants in the reactor, which has a negative effect on the overall conversion. The latter is greatly affected by the particle size of the packing materials. For example, due to the inhibition of the discharge volume by the solid packing,  $\gamma$ -Al<sub>2</sub>O<sub>3</sub> beads, both with and without supporting metals, were found to reduce the conversion of CH<sub>4</sub> and CO<sub>2</sub> compared to the plasma reaction in an empty reactor.<sup>[17d]</sup> A similar situation was observed in plasma-assisted nonoxidative CH<sub>4</sub> coupling over Ni-Fe mixed metal oxides.<sup>[42]</sup> The conversion over a catalyst with a Fe/Ni molar ratio of 3 was reduced by 15% as compared to that in an empty reactor. However, the catalyst can change the selectivity pattern. In this way, the catalyst directed the dry reforming reaction toward formaldehyde and methanol, which cannot be generated without a catalyst.<sup>[17d]</sup>

In most cases, the promotion of the reaction due to the catalytic activity and/or electric field enhancement by the support material could not compensate for the decreased conversion caused by the loss in reaction volume. Therefore, a better overall conversion was observed in reactors with high void spaces due to the plasma chemistry. For example, Ray et al.<sup>[43]</sup> demonstrated the performance of bimetallic catalyst for DRM, observing that the best performance over a Ni-Mn/ $\gamma$ -Al<sub>2</sub>O<sub>3</sub> catalyst was observed at a 25% catalyst loading (75% void space).

It is thus obvious that the overall performance is greatly affected by the particle size of the catalyst support and its dielectric properties. The dielectric constant of the microporous support, especially in the range between 4 and 200, has a large effect on the extent of plasma enhancement.<sup>[33a]</sup> The simulations showed that plasma is generated into pores larger than the Debye length,<sup>[34a]</sup> while typical commercial supports ( $\gamma$ -Al<sub>2</sub>O<sub>3</sub>, SBA-15, HZSM-5, CeO<sub>2</sub>, TiO<sub>2</sub>, multi-wall carbon nanotube) have pores with a mean size below 10 nm.

In order to resolve the issue of slow diffusivity in the mesoporous supports, several groups suggested the use of microporous supports with pore sizes that are larger than the Debye length, which is a measure of how far into the plasma the potential of a charged surface is observed. This length is ca. 600 nm at atmospheric pressure and temperatures close to

room temperature, which are typical plasma-catalytic conditions in many studies.

There are only a few recent works that systematically studied the effect of microporous supports with pore size in the range from 10 nm to 2  $\mu$ . These supports are not commercial products and should be made using templating synthesis. Wang et al.<sup>[44]</sup> used a modified Stöber method with silica spheres. The method was originally developed for the controlled synthesis of uniform submicron silica spheres and was recently expanded for the synthesis of microporous materials with different morphologies. Among others, ordered mesoporous silicas, with tunable pore size in the range of 8–10 nm and high surface area, were synthesized by the modified Stöber method.<sup>[45]</sup>

Not surprisingly, the method was also adopted for plasma-catalysis applications,<sup>[18a]</sup> as also discussed in the previous section. In this method, tetraethyl orthosilicate was added to an aqueous ammonia solution. The diameter of silica particles ranged from 10 to 2000 nm and was controlled by the ammonia concentration. The final product was obtained after centrifugation, drying at 80 °C for 24 h, followed by calcination at 800 °C for 12 h to interconnect the individual particles. In the next step, copper nitrate was dissolved between the pores, and the resulting sample was calcined to decompose the nitrate species. Finally, the silica template was removed by etching a NaOH solution to produce a 3D porous copper oxide.

The best conversion in plasma-catalytic DRM was observed over a sample with a mean pore size of 740 nm, even though this sample had a relatively small specific surface area of 2.0 m<sup>2</sup>·g<sup>-1</sup>. This is an order of magnitude smaller than the specific area of samples with a pore size of 100 nm. The advantage of the catalyst with a large pore size is that the plasma species formed inside the pores can reach the catalyst's active sites and react toward desirable products. A further increase in pore size would reduce the available surface area, and therefore, the contribution from the surface reactions decreases.

### 3.2. Reactor Design in Relation to the Catalyst and Electrode

There is a very large dependence on the performances in NTP plasma reactions of the type of reactors used, which also influence the different mechanisms present.<sup>[6b,9d]</sup> Among the different types of reactors/plasmas investigated, the most common are dielectric barrier discharges (DBDs), gliding arc (GA), gliding arc plasmatron (GAP), radio frequency (RF), microwave (MW) plasmas, and emerging technologies such as atmospheric pressure glow discharges (APGDs), nanosecond-pulsed discharges, and corona and spark discharges. They differ in how electricity is applied to generate plasma and the fluidodynamics of gas-discharge interaction, besides other aspects such as reactor, pressure, power, etc. However, only part of them could be effectively coupled with a catalyst, with DBD being the most used. There are several valuable maps of the scientific results for different types of reactions and reactors/plasmas investigated, evidencing the crucial impact of reactors on the performances (conversion, selectivity, energy efficiency).<sup>[6b,9a,46]</sup> However, a rationalization of all these results, and thus a reac-

tor design related to catalyst/electrode characteristics, is still challenging.

In plasma catalysis processes, both reactions in the gas phase induced by discharges and catalyst-induced reactions are present. Therefore, an optimal ratio between gas and catalyst volumes in the reactor must exist, although it is often not identified. In fluid bed plasma reactors,<sup>[47]</sup> the catalyst loading should be limited to 15%–20% of the total reactor volume, while in conventional catalytic fluid bed reactors, the catalyst loading is higher (typically 25%). In many cases, the catalyst volume can further be reduced by the application of thin catalyst coatings onto the inner reactor wall. Moreover, catalytic coatings directly onto plasma electrodes with different shapes (meshes, plates, fins) were also studied.<sup>[48]</sup> In most of these studies, the catalyst strongly influences selectivity. At the same time, it has little to moderate effect on the reactant conversion, which is obvious due to the limited volume occupied in the reactor.

In our recent study, it was shown that an Ir/TiO<sub>2</sub> catalytic coating can effectively enhance the rate of CO<sub>2</sub> hydrogenation in a DBD plasma reactor.<sup>[49]</sup> The Ir/TiO<sub>2</sub> coating with a thickness of 1.2 μm was deposited onto the inner wall of a quartz reactor (i.d.: 3 mm, o.d.: 5 mm) from a mixture containing a Ti precursor and a colloidal suspension of Ir nanoparticles by a combustion-evaporation method.<sup>[50]</sup> The IrO<sub>2</sub> phase formed in situ during the reaction was responsible for the high catalytic activity, which was more than 1.5 times higher than that in an empty reactor.

The existence of an additional surface route over the TiO<sub>2</sub> coatings resulted in a higher overall CO formation rate and a much higher CH<sub>4</sub> production rate, especially at higher CO<sub>2</sub> concentrations in the feed. The conversion in the CO<sub>2</sub> splitting reaction was enhanced when a few-micron mica layer (dielectric constant of 7) was deposited onto the ground electrode in a DBD reactor.<sup>[51]</sup> Mica is a generic name given to a group of complex hydrous aluminosilicates that have a plate-like porous structure. They have relatively large pores between the adjacent layers where plasma can be formed. With similar ideas, García-Moncada et al.<sup>[52]</sup> deposited a Pd/Al<sub>2</sub>O<sub>3</sub> catalyst coating on the inner wall of the coaxial DBD reactor for methane coupling in a 6% CH<sub>4</sub> in Ar gas mixture. They reported a rather constant CH<sub>4</sub> conversion of 34% at 2.8 W at room temperature with 6 vol.% CH<sub>4</sub> in Ar in the reactor with different thicknesses of the porous support. In contrast, the thickness of the catalyst layer strongly influenced the product distribution. It was concluded that the inner surface of the coating is not accessible to the active plasma species despite its porosity and that plasma-catalysis interactions take place on the outer surface.

Fluidized bed reactors represent an alternative configuration that allows relatively large void space in the discharge volume. In this configuration, the catalyst particles are fluidized by feeding gas with a velocity above the minimum fluidization velocity. The catalyst particle size can be decreased compared to fixed bed reactors, increasing the catalyst surface area and promoting high heat and mass transfer rates, which is important to avoid thermal runaways and local hotspots in the reactor.

Due to the difficulty of homogeneous fluidization in a tube of small diameter, only a few studies have reported this approach.<sup>[53]</sup> This is mainly due to the fact that particle–wall

interactions account for a considerable fraction of total (particle–particle and particle–wall) interactions, and they should be rated in the designs. The minimum gas flow velocity cannot also sustain a fluidized motion. The DRM reaction was dramatically promoted due to an extended surface area of powdered catalysts and their interaction with plasma-generated reactive species.<sup>[53a]</sup> The authors concluded that the entire outermost surface of γ-Al<sub>2</sub>O<sub>3</sub> support is responsible for the higher activity in the plasma–catalyst interaction. In a fixed bed reactor, however, plasma was limited near the contact points between alumina particles, which resulted in the deactivation of active sites.

A spouted-bed reactor combined with a gliding arc discharge was studied using a CH<sub>4</sub>/Ar mixture for CH<sub>4</sub> reforming.<sup>[54]</sup> The spouted bed configuration is one type of fluidized bed in which catalyst particles show circular movement in the inter-electrode space. Alumina-supported Ru, Rh, Pt, and Pd catalysts were studied at a temperature of about 100 °C. The plasma-induced synergy was, however, not confirmed in that study.

More recently, a rotating gliding arc plasma reactor combined with a spouted-bed section was studied for DRM.<sup>[55]</sup> Two supported catalysts, Ni/SiO<sub>2</sub> and Ni/Al<sub>2</sub>O<sub>3</sub>, were studied at a temperature of 220 °C. The CO<sub>2</sub> and CH<sub>4</sub> conversion was lower than in thermal catalysis at the same temperature. However, the syn-gas selectivity increased with the presence of a catalytic bed in the plasma zone. It was noted that the plasma introduced defect sites in the Ni nanoparticles, making them more electronegative, which may be responsible for higher selectivity.

A postplasma fluidized bed reactor is another possible configuration for plasma-catalysis reactors. The catalyst is placed downstream of the plasma zone to avoid catalyst deactivation. This configuration has a clear advantage in that warm plasma discharges do not damage the catalyst. However, the active species generated in the plasma zone cannot reach the catalyst, as the residence time needed for that is much longer than the characteristic lifetime of plasma species.<sup>[47]</sup> Gas-phase reactions dominate the reaction path in these reactors.<sup>[56]</sup> As a result, only relatively stable and less reactive intermediates can reach the catalyst surface. Yet the fluidized bed can also absorb a solid product, e.g., carbon, which is a byproduct of nonoxidative CH<sub>4</sub> decomposition.

The application of a fluidized bed reduces carbon deposition on other parts of the plasma system, elongating the productive reactor time between the cleaning cycles. In such an approach, a fluidized bed made of carbon particles can absorb the carbon product, which can lead to the possibility of creating a continuous operation via the constant removal of carbon particles from the reaction zone.

The main difficulty in the design of such reactors remains the need to enhance the radial gas–solid momentum transfer by the addition of a second (vertical) gas inlet and by the positioning of baffles of specific shapes.<sup>[47]</sup> Different structures are needed to redistribute the gas depending on the catalyst density and to provide better mixing of the gas phase and solid phases, improving the efficiency of the fluidized bed.<sup>[57]</sup>

Despite several studies that guide baffle addition into the fluidized bed, a systematic discussion on the baffle characteristic is still missing. Most related studies do not explicitly provide

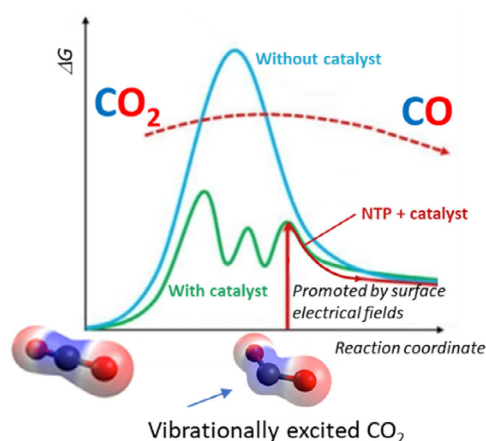


**Figure 3.** Conceptual illustration of the plasma catalysis mechanism to promote  $\text{CO}_2$  dissociation via vibrationally excited  $\text{CO}_2$ . An enhanced electrical field promotes this mechanism.<sup>[7]</sup>

engineering correlations needed for baffle design. Instead, they provide partial solutions for specific cases.

#### 4. Combining Plasma and Electro-/Photocatalysis

Combining plasma and electro-/photocatalysis is an emerging trend offering challenging possibilities.<sup>[58]</sup> When we refer to combining these technologies, the concept is based on the aspects commented on in the previous section. NTP generates excited molecules; thus, their interaction with a solid catalyst cannot be achieved via classical chemisorption, as in heterogeneous thermal catalysts. The excited molecule offers, in principle, a new lower transition energy path (Figure 3), thus changing the rate and selectivity.<sup>[7]</sup> However, it must be avoided that in the collision with the solid catalyst, the molecules lose their energy and excited state (or charge). Thus, a strategy is to use catalysts that are already charged on the surface, e.g., photo- and electrocatalysts. These charges create surface electric fields and localized phonons<sup>[2]</sup> that help in the synergic, rather than destructive, interaction between the NTP-excited species and the catalyst.

To fully exploit the synergies outlined above, the preferable configuration is the interaction of plasma-generated species with gas-phase type photo- and electrocatalysts.<sup>[59]</sup> In fact, the presence of a solvent/electrolyte could significantly alter the chemistry outlined above. However, it also opens new possibilities. Being a liquid electrolyte or solvent often present, these studies on the combination of NTP and photo-/electrocatalysts also address another emerging area, which is the catalytic chemistry at the plasma-liquid/solid interface. Plasma-liquid technologies are an increasingly important focus area,<sup>[58c,60]</sup> and they have recently opened new possibilities for catalysis. However, it is a highly complex topic because its understanding involves plasma science, fluid dynamics, heat and mass transfer, photolysis, multiphase chemistry, and aerosol science. Advanced diagnostics, modeling, and reactor design are necessary to address these challenges properly.

Plasmas interacting with liquids yield a highly reactive interfacial liquid layer and aerosol deriving from the processes driven by plasma-produced electrons, ions, photons, and radicals. Local electric fields influence these processes. This interfacial layer is different from that present in conventional electrochemical systems, where a solid electrode directly generates solvated electrons in an electrolyte solution. The high-power density in plasmas enables exceptionally large fluxes of electrons, some having high energies of up to 10 eV or more. This fact leads to a high concentration of (solvated) electrons in a near plasma-liquid interfacial region with a thickness of up to a few tens of nm.<sup>[60]</sup> Similarly, the interfacial region in photocatalytic reactions is expected to be drastically altered, but it is an unexplored area.

It is evident how this possibility drives significant innovation to intensify not only plasma but also electrolysis processes. However, it also brings complex challenges to solve. Thus, it may be necessary as a first stage to consolidate the evidence of how it may bring a new dimension to reactive catalysis studies in order to stimulate modeling and experimental characterization (diagnostic) studies in the area and also raise the industrial interest, which is now somewhat skeptical of the possibility of scaling up these approaches. We will comment on some examples in this field to remark on the possibilities, although the aim is not to review the field systematically.

Often referring to combining NTP and electro-/photocatalysts in the literature, the plasma is only used to induce modifications in the catalysts, for example, to create defects, metastable surface species, or electronic modifications.<sup>[58a]</sup> In these cases, the plasma is only a pretreatment or sometimes an in situ way to modify the catalysts dynamically. Even if the use of NTP in the modification/pretreatment of catalysts (including thermal ones) is an area covered by many studies,<sup>[61]</sup> this is mainly an academic activity, still with limited possibilities for industrial application.

Nevertheless, many possibilities are offered, including aspects such as low-temperature routes to decompose or generate active species. The NTP flux and generation of a strong local electric field induce different types of nucleation and crystal growth. It is possible to synthesize electro-/photocatalysts on a thermolabile substrate. Plasma treatment can induce etching, exfoliation, and other permanent effects in mild conditions, which are important for photo-/electrocatalysis. NTP can be used to regenerate deactivated catalysts by removing carbon deposits. Even with these valuable possibilities, we discuss only examples of true synergetic interaction between NTP and electro-/photocatalysis here.

Note that understanding plasma catalysis properly and its interaction is highly challenging, as commented in the previous sections. Often, the catalyst only induces a change in the physics of the plasma generation mechanisms rather than creating effective novel catalytic paths. In photo-/electrocatalysis, there is an additional degree of complexity with respect to thermal catalysis. Thus, the interaction with plasma introduces a further degree of complexity, reaching a level often above our understanding capability. It is thus an area still largely phenomenological, and often, the interpretation given to explain the behavior is not sufficiently proven.

Amal and collaborators<sup>[62]</sup> were among the first to present a hybrid plasma electrocatalytic process for sustainable ammonia production. They couple plasma-driven  $\text{NO}_x$  generation and their electrocatalytic reduction to ammonia. This approach is sequential, i.e., a dual in-series reactor is used. This approach allows, in optimal conditions, to achieve a rate of  $23.2 \text{ mg h}^{-1}$  of ammonia production. However, this approach combines two technologies rather than exploiting a synergy between plasma and photocatalysis.

Meng et al.<sup>[63]</sup> presented an example of plasma-assisted enhancement in photocatalytic behavior for the challenging reaction of converting  $\text{CH}_4$  to higher hydrocarbons. This reaction has a relevant potential impact on the utilization of natural gas, particularly stranded resources. Note that UV radiation can be self-generated by nonthermal DBD plasma.<sup>[64]</sup> Thus, in principle, NTP can be a way to generate an additional light source locally. It is thus important to conduct tests to analyze whether this is important or not.

Photooxidative dehydrogenation of  $\text{CH}_4$  generates C2 hydrocarbons, with a high selectivity of up to 90% for ethane.<sup>[59d,65]</sup> However, a fast deactivation is present. Meng et al.<sup>[63]</sup> showed that for a Ti-Ga/UZSM-5 catalyst, the illumination of the sample increased by about 15% the  $\text{CH}_4$  conversion obtained in NTP conditions. Still, activity is zero for only the photocatalysis case on their materials. Light irradiation (during NTP operations) also influences product distribution and the reduction of coke formation. Thus, the combination of light/photocatalyst promotes NTP  $\text{CH}_4$  conversion. However, the chosen photocatalyst is inactive in the photoconversion of  $\text{CH}_4$ , which is different from other photocatalysts, even  $\text{TiO}_2$ , which is active but easily deactivates. Can NTP be a way to make stable photocatalyst behavior instead? Turning the attention from the light promotion of the plasma effect to how the photobehavior can be promoted by plasma could be necessary. In plasma reactions, the nature of discharges can be drastically influenced by the nature of materials used in the dielectric barrier or the void space above it. Modifications in the photocatalyst can alter its ferromagnetic properties. Thus, the changes may not be associated with chemical changes in the mechanism but rather with modifications in the physics of plasma processes (e.g., discharge modes), as also discussed earlier in this paper (i.e., the catalysts act as plasma modifiers).<sup>[15a]</sup>

Saoud et al.<sup>[66]</sup> investigated the combined plasma-photocatalysis in an annular DBD plasma reactor illuminated by a UV lamp and using a  $\text{TiO}_2$  photocatalyst as the dielectric material. They studied the oxidative degradation of pollutants. The objective was to arrive at a pilot unit to clean the air in the livestock building. When either photocatalysis or plasma alone was used, the degradation yields were 29% and 36% for  $\text{NH}_3$  and 37% and 42% for propionaldehyde, respectively. Combining plasma and photocatalysis, 72% and 83% degradation yields for  $\text{NH}_3$  and propionaldehyde, respectively, were obtained. There is thus a clear synergy in combining the two approaches.

Ammonia and propionaldehyde or other chemicals<sup>[67]</sup> could be effectively removed, with a significant synergy in coupled plasma/photocatalysis (Figure 4), particularly at the lower SE (specific energy) values. On the other hand, combined

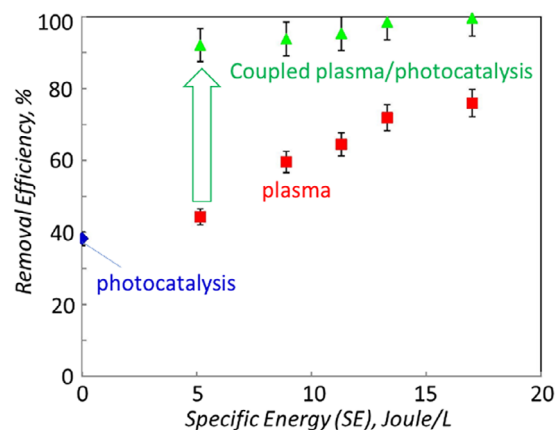


Figure 4. Dependence on SE of the removal efficiency of isovaleraldehyde in photocatalytic, plasma, and coupled plasma/photocatalysis experiments. Adapted with permission from Ref. [67]. Copyright Elsevier, 2014.

DBD plasma/photocatalysis enhances  $\text{CO}_2$  selectivity significantly compared to DBD plasma alone. The interpretation is that plasma enhances the formation of hydroxyl radicals ( $\cdot\text{OH}$ ), e.g., the oxidant species generated in photooxidation processes. However, the mechanisms of promotion are not defined or demonstrated, nor are alternative possibilities investigated. In addition, the energy efficiency in DBD reactors is rather low.

Mei et al.<sup>[64]</sup> showed that the combination of plasma with  $\text{BaTiO}_3$  and  $\text{TiO}_2$  catalysts significantly enhances the conversion of  $\text{CO}_2$  (in splitting to  $\text{CO}$  and  $\text{O}_2$ ) and the energy efficiency by a factor of 2.5 compared to the plasma reaction in the absence of a catalyst. However, the photocatalyst also modifies the type of discharge. Thus, it is challenging to understand whether there is a physical effect on the type of plasma discharge or an effective plasma-photocatalysis synergy.

A hybrid plasma photocatalysis system for converting  $\text{CO}_2$  and  $\text{CH}_4$  to syngas was studied by Chung et al.<sup>[68]</sup> They found a 42% enhancement, which they attributed, although not fully proven, to an enhanced lifetime of electron-hole pairs in the photocatalyst. The enhancement (in a spark discharge reactor packed with  $\text{LaFeO}_3$  photocatalyst) increases the syngas generation rate from 13.0 to 18.5 mol per kilowatt-hour, i.e., 42% of enhancement.

These limited examples show the potential synergy of coupling plasma and photocatalysis to develop novel challenging routes or improve the existing ones. However, it also reveals that there is a lack of understanding and consideration of all the possible mechanistic alternatives, including plasma physics. How to realize the coupling, what are the possibilities to promote the synergy and for which reactions, and how to design an optimal reactor to exploit synergy are, among others, open questions.

The combination of plasma and electrolysis/electrocatalysis also presents many challenges. Plasma-assisted nitrogen fixation is one of the valuable directions explored.<sup>[69]</sup> Kumari et al.<sup>[70]</sup> used a nitrogen plasma to feed the cathode side of an electrolyzer and thus provide plasma-activated  $\text{N}_2$  species to the electrocatalyst surface. They observed a 47% increase in ammonia formation at an applied bias of  $\sim 3.5 \text{ V}$  across the electrolyzer compared to the case without bias. This applied bias

is larger than usual, but current densities (around  $200 \text{ mA}\cdot\text{cm}^{-2}$ ) are larger than in usual electrocatalytic  $\text{NH}_3$  synthesis from  $\text{N}_2$ .<sup>[71]</sup> However, Faradaic efficiency was not reported, nor were other important aspects such as energy efficiency, etc. The mechanism suggested, but not proven, is that vibrationally excited  $\text{N}_2$  species electrochemically react with  $\text{H}^+$  atoms on the cathode. The influence of the nature of the latter was also not determined.

Peng et al.<sup>[72]</sup> study the plasma-assisted  $\text{N}_2$  fixation to  $\text{NH}_3$  at the interface between water and spray-type jet plasma. There is a twofold increase in the rate of  $\text{N}_2$  fixation, with the formation of ammonium ions and nitrate/nitrite, which are predominant. The mechanism suggested is the electron excitation of the  $\text{N}_2$  gas molecule to form monoatomic nitrogen radicals together with hydroxyl and hydrogen radicals formed by the electron excitation of the vaporized water. The latter two radicals react with the N species to form  $\text{NH}$  and  $\text{NO}$ , respectively, and then are further converted to ammonia (ammonium ions in water) and  $\text{NO}_x$  (nitrite/nitrate in water). There are doubts and many unproven aspects to this mechanism. However, these results indicate two points: i) there is an important plasma-water (electrolyte) chemistry to consider in analyzing the results of plasma-assisted electrolysis, and ii) the electrocatalyst and the associated potential/electrical field may significantly influence this chemistry, in addition to influencing the plasma physics.

Hawtof et al.<sup>[73]</sup> used a different approach in developing a hybrid plasma-electrolytic system for  $\text{N}_2$  fixation. They also studied the interaction of an  $\text{N}_2$  plasma with water but applied a potential between the plasma-jet-type electrode and a metal-foil electrode immersed in the water solution. They claim record-high Faradaic efficiency (up to 100%) and good ammonia formation (in the range of 0.3 mg; total  $\text{NH}_3$  produced after 45 min at 6 mA and pH 3.5). The suggested mechanism is the generation of vibrationally excited  $\text{N}_2$  in the plasma and hot electrons, which generate solvated electrons in water. These species react at the immersed cathode to generate ammonia, although the mechanism has not been clarified. A better understanding is necessary, including the role of the electrode and how to design a more efficient and scalable reactor. The mechanistic key is the role of solvated electrons<sup>[74]</sup> and their reduction of protons to hydrogen radicals, which react with  $\text{N}_2$ . In this case, the chemistry at the aerosol interface between the gas plasma jet stream and the water is neglected. In contrast, in other cases, this is the dominant effect considered, as commented before.

This chemistry can also be used in other challenging reactions, one of them being  $\text{H}_2\text{O}_2$  direct synthesis,<sup>[75]</sup> for the variety of uses of hydrogen peroxide, from clean chemical production to water and soil remediation. Although  $\text{H}_2\text{O}_2$  direct synthesis is an active research area, both by electrocatalytic and plasma routes, their coupling to exploit synergies has not yet been explored.

There are other potential areas for combining plasma and electrocatalysts, such as  $\text{CO}_2\text{RR}$  (electrocatalytic reduction of  $\text{CO}_2$ ). However, attempts in this direction still refer only to a plasma pretreatment of the electrocatalyst<sup>[76]</sup> or to integrating an electrochemical stage of oxygen separation after the plasma-induced splitting of  $\text{CO}_2$ .<sup>[58b]</sup> There is a potential instead to stream the  $\text{CO}_2$  plasma to water at an anode, producing potentially methanol or other alcohols with intensified production

with respect to conventional electrocatalytic  $\text{CO}_2\text{RR}$ . However, this possibility is not yet reported in the literature.

The use of combined plasma-electrolysis for oxygen evolution reaction (OER) is also still limited to a plasma pretreatment to modify the anode characteristics, such as conductivity, defects, and coordinatively unsaturated species.<sup>[77]</sup>

Another relevant direction is to produce  $\text{H}_2$  by plasma-driven solution electrolysis,<sup>[78]</sup> as an advance to plasma-only methods.<sup>[79]</sup> Plasma-driven solution electrolysis can be anodic or cathodic, but the latter is preferable. There is complex chemistry and physics: Faradic electrolysis, Joule heating, solvent evaporation, gas-vapor envelope formation, ionization of the mixture, and electrical discharge induction. Thus, a dependence, often not linear, from many parameters, such as the electrolytic solution's temperature, electrolytic solution concentration, the discharge electrode's immersion depth, organic additive presence, and applied voltage. However, enhancements by a factor of four have been demonstrated compared to electrolysis.<sup>[78]</sup> Reactor configuration is also crucial.<sup>[80]</sup>

Although not exhaustive, these examples show that there is good potential in overcoming some of the limits in photo/electro processes and vice versa, in terms of process intensity from one side and controlling selectivity and increasing energy efficiency from the other side by coupling them with plasma. It is, however, a very complex topic with still too limited advances in understanding and rationalizing, as well as modeling, the phenomena present. The presence of a solvent/electrolyte increases further complexity but also offers new possibilities, as outlined in the examples discussed.

## 5. Sustainability and Perspective of Translation From Lab to Applications

This section analyzes the gap and opportunities for plasma-based chemical production to become a "near-transition" emerging technology. Gap refers to the general lack of industrial demonstration of plasma applications despite promising pilot applications. This is due to intrinsic energy disadvantages, which, however, have been continuously improved over the past two decades. One of the rare exemptions is scaled-up plasma reactor systems for environmental and energy applications, including the treatment of exhaust gases from fossil-fueled combustors and combustion engines.<sup>[81]</sup>

Due to the gap in industrial use, plasma processing has the developmental status of proof-of-concept emerging technology, for which environmental assessment is typically not well developed (Figure 5). Life-cycle analysis (LCA) communicates with and attracts societal interest groups that can promote industrially, mainly academics and some ecologists. The opportunity is to improve the environmental and cost footprint of plasma-assisted processes along three main factors, which are (i) plasma energy efficiency, (ii) use of renewable energy, and (iii) recycling of nonprocessed material.

Plasma processing needs to be propelled into the category of "near-transition" emerging technologies, being on the verge

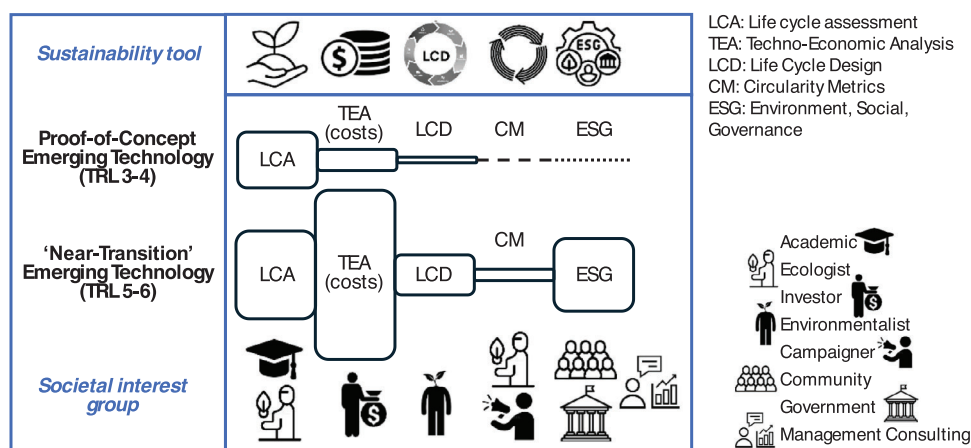


**Figure 5.** Status of diverse sustainability assessments for a proof-of-concept emerging technology (plasma) versus a “near-transition” emerging technology (hydrogen). The height of the square for each assessment marks semi-quantitatively the coverage in the scientific literature (number of papers), as per a quick Google Scholar search. The diverse sustainability assessments reach certain interest groups, as depicted, which is their target audience.

of global industrial scale, because they communicate with and attract societal interest groups of breadth (origin, motivation, ability) that can promote industrial transition (Figure 5). This category belongs to the generation of hydrogen by splitting water or the conversion of  $\text{CO}_2$  to valuable products, which have managed to attract manifold sustainability assessments.

Many plasma sustainability studies rely on laboratory reactors, while crucial aspects of upvaluing sustainability studies are scaling up and process design aspects. Therefore, this section focuses, in a combined fashion, on reviewing sustainability and scaling up its ability to translate industrially.

Plasma can emerge to a “near-transition” position by (a) focusing on markets that suit the technology (“prospective”), which are impacted by the above-given plasma levers (i)–(iii), (b) developing its markets and windows of business (“tailored”), and (c) providing its sustainability benefits in a language that the business and sustainability world understands beyond academic curiosity. The following discussion is structured along (a)–(c) aspects. The aim is to provide examples to guide further studies, while a detailed discussion of each case is out of the scope.

### 5.1. Plasma Sustainability in Prospective Markets

Plasma needs to generate benefits in the material/waste valorization to counterbalance its energy disadvantage.<sup>[82]</sup> Thus, the key is the full conversion of materials and/or avoidance of waste when conventional processes produce a lot of waste. Materials-dominated process scenarios are, for example, the pollutant decomposition of industrial waste gases, including airborne contaminants such as nitrogen and sulfur oxides ( $\text{NO}_x$  and  $\text{SO}_x$ ) and volatile organic compounds (VOC).<sup>[82]</sup> More benchmarking of plasma technologies to industrial technologies is needed in material/waste-dominated markets. An LCA study showed that the environmental impact of electron beam flue gas treatment (EBFGT), one of the advanced plasma methods, was similar to adsorption.<sup>[82]</sup> At the same time, the DBD approach was significantly better than biofiltration. It also lowers the impact on

waste conversion compared to conventional wet flue gas desulfurization with selective catalytic reduction (WFGD + SCR).<sup>[82]</sup> Yet, applying plasma has the benefit of co-generating marketable byproducts.

The thermochemical upcycling of the plastic industry is an ideal example of implementing and co-valorizing recycling in an end-of-life fashion, finally leading to a carbon-negative footprint. A plastic-recycling process has been designed to oxidatively depolymerize waste polyolefins in a  $\text{CO}_2$  plasma to produce oleochemicals and hydrocarbon chemicals in a one-stage process at large reactivity.<sup>[83]</sup> The environmental benefits are garnered at atmospheric pressure operation, without the need for solvent or catalyst, and with the use of  $\text{CO}_2$  as an oxidant. 97.6% of fatty alcohols could be produced within minutes. LCA computes the global warming potential between  $-3.1$  and  $-3.3$  kg  $\text{CO}_{2e}$  per kg of plastic. A techno-economic analysis (TEA) calculates that 43% of waste plastics need to be converted to result in a viable industrial process.

As an example of a materials-based process, 97% of  $\text{CO}_2$  emissions were omitted from a plasma-assisted  $\text{CO}_2$  splitting process to CO (and  $\text{O}_2$ ) in a best-case scenario.<sup>[84]</sup> At an energy efficiency of 1.7%, the  $\text{CO}_2$  conversion was 40.2% at the price of diluting the reactant stream and using costly argon gas to stimulate plasma excitation. The use of photovoltaic energy is key to sustainability gains.

Fertilizers are key materials produced by plasma. For a plasma process to produce nitric acid, the LCA-predicted global warming potential decreased by 19% compared to the traditional nitric acid production when considering the recycling of the tail gas and the use of solar energy.<sup>[85]</sup>

### 5.2. Plasma Sustainability in New Tailor-Made Markets

Plasma processing cannot rely solely on the use of a few prospective markets. It needs to explore new windows of opportunity and new process windows proactively. This demands a move toward a technology and product-delivery position that

the current industry fails to occupy. Small-scale units, i.e., a distributed production suited for fast changes in demand, are a major current play for emerging plasma technologies.

The ammonia (NH<sub>3</sub>) production via the Haber–Bosch (HB) process consumes large energy that is executed only in a small number of countries in world-scale plants of the largest productivity.<sup>[86]</sup> The estimated environmental costs for the NH<sub>3</sub> industry in Australia amount to about US\$5 billion per year. Local plants next to farmers can reduce environmental impacts, as well as reduce storage, shortage risks, and price volatility of fertilizers. LCA studies and cost analysis accounting for decentralization and local benefits by minimizing transportation prove the advantages of this solution.<sup>[86]</sup> Different scales of storage and transportation were computed down to a regional and even local scale of plasma-assisted production of NH<sub>3</sub> fertilizers.

Local production based on emerging technologies alone is not cost-effective and relies on the internalization of covalorization and environmental impacts into economic benefits. For plasma-assisted NH<sub>3</sub> production, byproducts, such as steam, oxygen, or carbon black, can be utilized for internalization.<sup>[86]</sup> A plasma-assisted ammonia process was computed to be cost-competitive at \$222/tonne NH<sub>3</sub> when considering cost internalization.<sup>[86]</sup>

Applying the same internalized cost computation, electrolyzer-HB plants would operate at costs of \$114/tonne NH<sub>3</sub>, which is a consequence of their great energy efficiency and oxygen co-generation value. Without internalization, the external costs of nonthermal and thermal plasma processing are much higher, amounting to \$4200 and \$9500/tonne NH<sub>3</sub>, respectively. This is majorly caused by the costs of purchasing solar panels to utilize renewable energy.

### 5.3. Plasma Sustainability Methodology

Emerging technologies suffer from being refrained from informing industrial decision-makers; they are “not on the radar.” Plasma sustainability reports need to include new kinds of sustainability methodologies that can reach those that can change the industry. The current sustainability assessments of plasma technology are too much centered around LCA, which is an academic and recondite tool. More simple cost analyses (TEA) could break this complexity, yet they are available to a lower degree for plasma processing. Studies using circular economy metrics are closer to the needs and tangibility of governments, intergovernmental organizations (e.g., the United Nations), and companies. Yet, the key to reaching industrial decision-makers and investors would be an assessment of social and governance values, and the widely established tool here is Environment, Social, and Governance (ESG).

Plasma sustainability also suffers from a too narrow-minded process viewpoint, as it is often based on factory-gate-to-factory-gate LCA and then does not account for a holistic process view by considering the ecological backpack (cradle-to-gate) or ecological downstream benefits/end-of-life and product-end-of-life (gate-to-grave).<sup>[87]</sup> A holistic LCA assessment has been conducted for the nonthermal plasma-based methane dry reforming

(NTP-DRM) for the generation of hydrogen. The best environmental performance was found for the use of microwave and pulsed plasmas, which outperformed DBD plasma.

Life cycle thinking (LCT) is another tool that is closer to the specific kind of information that reaches decision-makers. LCT involves cost assessment as per life cycle cost (LCC) and as a “soft spot” social assessment (social-LCA, SLCA), both of which are scarcely reported for plasma processes. An LCT study on plasma gasification was conducted to convert solid waste residues from open dumps or landfills into energy, coined “Waste-to-Energy” (WtE).<sup>[88]</sup> This study included LCC and SLCA.

### 5.4. Process Development and Scale-Up: From Lab to Application

Conventional-style process screening also uplifts plasma processing, as reported by a sensitivity analysis for the plasma-based synthesis of nitric acid, which conducted scenario variation of yield, power usage, recycling, and energy recovery.<sup>[85]</sup> Renewable energy sources can massively change plasma sustainability, as demonstrated by an ex-ante LCA assessing a proposed large-scale process design for plasma-based synthesis of nitric acid.<sup>[85]</sup>

The conventional style in process design (and scale-up) is to optimize reactor design and geometry. Two plasma-based reactors for nitrogen fixation were compared, including a small arc reactor and a large one.<sup>[89]</sup> The small reactor has a low energy cost of 2.8 MJ mol<sup>-1</sup> for a NO<sub>x</sub> concentration of 1.7% (20 ln·min<sup>-1</sup>), manufacturing 33 g·h<sup>-1</sup>. The measured energy cost is close to the computed minimum thermodynamic equilibrium at atmospheric pressure. The high flow rates typical for the large reactor decrease the NO<sub>x</sub> concentration at similar energy costs. The key to further optimization of scale-up is the geometrical configuration of the arc and, more generally, the reactor configuration, plasma geometry, and power deposition. The performance of the large reactor at 80 g·h<sup>-1</sup> and 2.9 MJ·mol<sup>-1</sup> suffers from the contraction of the plasma, and a solution was demonstrated by changing to a torch configuration.

As a more sophisticated process approach, chemical process settings outside the mere plasma process can have a significant impact on the overall plasma-LCA performance. Steam use is the “energy digit” in chemical processes and a known main factor in the LCA output, as shown by the high sensitivity to natural gas reported in the uncertainty analysis.<sup>[87]</sup> The use of renewable energy sources, as demonstrated in the same study, can largely improve the environmental outcome of plasma-assisted NTP-DRMs, specifically their global warming potential. With a view on upstream process, and process-internal settings, various options for purge stream utilization and electricity sources (natural versus shale gas) were considered for the plasma-based generation of ethylene from methane.<sup>[90]</sup>

As another sophisticated process approach, plasma process development might profit from sequential (two-step) processing rather than completing chemistry directly (one-step). Natural gas was converted to ethylene in one step by a plasma-assisted process and benchmarked to a two-step process with first the conversion to acetylene and then an acetylene-to-ethylene

hydrogenation.<sup>[90]</sup> The two-step process has a lower CO<sub>2</sub> emission than the one-step process using renewable energy (wind) and utilizes the purge stream as the co-generated product. The use of shale gas reduces CO<sub>2</sub> emissions by comparison to natural gas, resulting in emissions similar to those of traditional naphtha cracking.

The plasma treatment for the selective catalytic reduction was compared to the NO<sub>x</sub> decomposition (De-NO<sub>x</sub>) and wet lime-gypsum SO<sub>x</sub> decomposition.<sup>[90]</sup> As a solution for uplifting plasma treatment, integration with industrial techniques of known low power consumption was proposed.

Given that the plasma process is optimal, it needs to be scaled to industrial productivity. This was recently demonstrated for plasma-based CO<sub>2</sub> splitting by placing several gliding arc plasma reactors in parallel (multi-reactor gliding arc plasma-tron: MR-GAP).<sup>[91]</sup> The concept of numbering up (“equaling up”) or, generally, the capability to produce “at scale” has transitioned microreactor processing and flow chemistry to industrial scale.<sup>[92]</sup> Numbering up was only successful in conjunction with a smart scale-out of dimensions from the micro- to the milli-scale. The question is if this numbering-up/scale-out concept is also amenable to plasma processing with similar prospects. The computation of scaling out a micro-plasma reactor to a few millimeters’ channel diameter resulted in high energy efficiency for CO<sub>2</sub> splitting.<sup>[93]</sup>

The feasibility of numbering up plasma reactors is inevitably connected with the ability to use the same power supply. Learning can be taken from flow chemistry, which is needed to minimize the number of pumps when numbering up microreactors. The costly “feed equipment for both plasma and flow chemistry cannot be numbered” but needs to be “scaled” up. Against that backdrop, three different types of power supplies were compared for the plasma-assisted conversion of water to hydrogen peroxide.<sup>[94]</sup> Individual, independent power supplies for each reactor were compared to capacitive AC and capacitive DC supplies that, as central “feeds,” suit the operation of many plasma reactors in parallel.

Scale-up is never easy, yet definitively, it is not straightforward when approaching true innovations in the plasma itself, but it is worth undertaking to unleash this innovation potential. Surface plasmas at a solid-gas interface are considered more powerful and energy-efficient than conventional plasmas for the decontamination of pollutants such as nitrogen oxide (NO).<sup>[95]</sup> Yet, the surface-generated benefit causes a problem when numbering up. Surface-induced charges might interact with the connected discharge chambers. A solution was developed for the prevention of unwanted interaction, using a conductive foil that acts as a barrier between the individual plasma (chamber) reactors. As an additional, unforeseen benefit, the electrical power was increased 40 times while keeping conversion. The energy effort for 50% NO degradation is 60 eV/molecule, and the energy constant of 0.02 L/J was not changed by shielding.

Learning for nonthermal plasmas can also be taken from the established scale-up of thermal plasmas. Microwave plasmas for industrial decarbonization transfer the electromagnetic field energy to the particles through collisions to create high-density plasmas.<sup>[96]</sup>

## 6. Conclusions and Recommendations

Chemical production is facing major challenges not only in addressing climate change but also in competitiveness and sustainability that will determine a transformation of the modalities of chemical production, which are often underestimated. New technologies, based on the use of local resources, including energy, should be developed. Addressing these challenges requires the development of innovative solutions, with plasma catalysis being among them.

This perspective summarizes various years of studies and discussions made in the frame of the ERC Synergy project SCOPE dedicated to the above aspects. However, it does not aim to overview the project results but rather use them in combination with literature indications to outline the emerging trends and present gaps to pass from a research area to a key technology to develop sustainable production and associated changes required in the modalities of production. The perspective thus aims to offer a vision of the future for plasma catalysis and its role in facing societal challenges.

While major progress in plasma catalysis modeling has been achieved in the past decade, both for studying the detailed chemical kinetics (in the plasma and at the catalyst surface) and for describing plasma streamer propagation inside plasma catalysis reactors, there are still major knowledge gaps in plasma catalysis, to design the optimal catalyst (both in terms of chemical and physical-electrical effects on the plasma), as well as the optimal plasma reactor geometry, and to tune the plasma operating conditions, in order to fully exploit the plasma-catalyst synergy, which is nowadays often lacking.

Briefly speaking, the catalyst should not quench radicals (thus acting as an “anti-catalyst”), which is now suggested to be the case for metal catalysts, but should really promote the reactions, i.e., operate in synergy with the NTP plasma. Alternatively, the plasma conditions should be tuned to maximize excited species, which can reduce the dissociation barrier at the catalyst surface. And last but not least, plasma-catalyst contact should be greatly improved. Hence, there is a clear need for detailed, fully coupled plasma and surface chemical kinetics models, if possible, integrated into 3D self-consistent fluid dynamics models, that fully couple the plasma and catalyst surface chemistry with the gas flow dynamics, heating, plasma electrical behavior (such as streamer propagation), and species transport to and from the catalyst surface.

Furthermore, advanced reactor and electrode designs are crucial to making plasma catalysis technologies effective. Among the various aspects highlighted in this section, some of them should be marked again:

- The gas phase to catalyst volume ratio in plasma reactors should be optimized. Thin catalytic layers and fluidized bed reactors provide such a possibility.
- Porous supports with a pore size >600 nm are needed for efficient plasma-catalysis interaction.
- The thickness of porous catalyst coatings does not improve the reactant conversion, yet it influences the selectivity.

These are other important elements in reactor, catalyst, and electrode design. Certainly, the reactor design has a crucial role, as demonstrated by the very large dependence on its performances from the reactor itself. However, this is related to the combination of realizing efficient discharges and the fluidodynamic interaction of the gas phase with them, as well as the minimization of the backreactions. However, this is true for plasma-only reactions, while in plasma catalysis (the focus of the discussion here), the situation is different. First, the choice of the possible type of reactors is limited. It is necessary to avoid the catalyst being destroyed by interaction with the plasma while at the same time ensuring that the short-lived excited species generated in the plasma arrive rapidly at the catalyst surface. Second, the catalyst/electrode may also significantly alter the mechanism of the generation of plasma and, thus, the generated excited species. In plasma catalysis, an integrated reactor/electrode/catalyst design is crucial to optimize the performances, but the search for new types of reactors and nanostructured electrodes is equally critical.

Combining plasma with other technologies based on renewable energy, e.g., photo- and electrocatalysis, offers many possibilities to develop innovative synergetic technologies, even if this is a topic only starting to be explored. We have provided some examples that show the disruptive possibilities offered by a better understanding of the underlying processes and how to optimize them.

Finally, the section on sustainability and perspective of translation from lab to applications offers unconventional indications and case studies, remarking on the relevance of these studies from one side and the need to develop innovative analysis tools beyond those in use.

In conclusion, we believe that this perspective offers new clues to understand better the prospects of plasma catalysis and its role in transforming changes in chemical production.

## Acknowledgements

This research was supported by the European Research Council (ERC) under the European Union's Horizon 2020 research and innovation program (grant agreement no. 810182–SCOPE ERC Synergy project).

Open access publishing facilitated by Università degli Studi di Messina, as part of the Wiley - CRUI-CARE agreement.

## Conflict of Interests

The authors declare no conflict of interest.

## Data Availability Statements

The data that support the findings of this study are available on request from the corresponding author. The data are not publicly available due to privacy or ethical restrictions.

**Keywords:** Combining plasma with electro-/photocatalysis · Electrode and reactor design · Plasma catalysis · Plasma modeling challenges · Sustainability plasma processes

- [1] a) E. T. C. Vogt, B. M. Weckhuysen, *Nature* **2024**, *629*, 295–306; b) G. Centi, S. Perathoner, *Green Chem.* **2022**, *24*, 7305–7331; c) G. Papanikolaou, G. Centi, S. Perathoner, P. Lanzafame, *ACS Catal.* **2022**, *12*, 2861–2876.
- [2] a) G. Centi, S. Perathoner, *Catal. Today* **2023**, *423*, 113935; b) G. Papanikolaou, G. Centi, S. Perathoner, P. Lanzafame, *Chin. J. Catal.* **2022**, *43*, 1194–1203.
- [3] a) A. I. Stankiewicz, H. Nigar, *React. Chem. Eng.* **2020**, *5*, 1005–1016; b) L. Zheng, M. Ambrosetti, E. Tronconi, *ACS Eng. Au* **2024**, *4*, 4–21; c) H. Yang, I. Nuran Zaini, R. Pan, Y. Jin, Y. Wang, L. Li, J. J. B. Caballero, Z. Shi, Y. Subasi, A. Nurdiawati, S. Wang, Y. Shen, T. Wang, Y. Wang, L. Sandström, P. G. Jönsson, W. Yang, T. Han, *Nat. Commun.* **2024**, *15*, 3868.
- [4] a) A. Ramanujam, G. E. Constante-Flores, C. Li, *AIChE J.* **2023**, *69*, e18265; b) M. Patrascu, *Chem. Eng. Process. Process Intensif.* **2023**, *184*, 109291.
- [5] a) A. Bogaerts, G. Centi, V. Hessel, E. Rebrov, *Catal. Today* **2023**, *420*, 114180; b) G. Centi, S. Perathoner, C. Genovese, R. Arrigo, *Chem. Commun.* **2023**, *59*, 3005–3023; c) G. Papanikolaou, G. Centi, S. Perathoner, P. Lanzafame, *Curr. Opin. Green Sustain. Chem.* **2024**, *47*, 100918.
- [6] a) A. Fridman, *Plasma Chemistry*, Cambridge University Press, Cambridge **2008**; b) A. Bogaerts, G. Centi, *Front. Energy Res.* **2020**, *8*, 111.
- [7] V. Longo, G. Centi, S. Perathoner, C. Genovese, *Curr. Opin. Green Sustain. Chem.* **2024**, *46*, 100893.
- [8] a) N. Belkessa, A. A. Assadi, A. Bouzaza, P. Nguyen-Tri, A. Amrane, L. Khezami, *Environ. Res.* **2024**, *257*, 119333; b) V. Maslova, R. Nastase, G. Veryasov, N. Nesterenko, E. Fourné, C. Batiot-Dupeyrat, *Prog. Energy Combust. Sci.* **2024**, *101*, 101096; c) E. C. Neyts, K. Ostrikov, M. K. Sunkara, A. Bogaerts, *Chem. Rev.* **2015**, *115*, 13408–13446; d) B. Loenders, R. Michiels, A. Bogaerts, *J. Energy Chem.* **2023**, *85*, 501–533; e) L. Lefferts, *Angew. Chem. Int. Ed.* **2024**, *63*, e202305322; f) G. Giammaria, G. van Rooij, L. Lefferts, *Catalysts* **2019**, *9*, 185.
- [9] a) R. Snoeckx, A. Bogaerts, *Chem. Soc. Rev.* **2017**, *46*, 5805–5863; b) M. Scapinello, E. Delikonstantis, G. D. Stefanidis, *Chem. Eng. Process. Process Intensif.* **2017**, *117*, 120–140; c) J. Hong, S. Prawer, A. B. Murphy, *ACS Sustainable Chem. Eng.* **2018**, *6*, 15–31; d) A. Bogaerts, E. C. Neyts, *ACS Energy Lett.* **2018**, *3*, 1013–1027; e) K. H. R. Rouwenhorst, Y. Engelmann, K. van't Veer, R. S. Postma, A. Bogaerts, L. Lefferts, *Green Chem.* **2020**, *22*, 6258–6287; f) S. Liu, L. R. Winter, J. G. Chen, *ACS Catal.* **2020**, *10*, 2855–2871; g) K. H. R. Rouwenhorst, J. Jardali, A. Bogaerts, L. Lefferts, *Energy Environ. Sci.* **2021**, *14*, 2520–2534.
- [10] a) E. C. Neyts, A. Bogaerts, *J. Phys. D Appl. Phys.* **2014**, *47*, 224010; b) J. C. Whitehead, *J. Phys. D Appl. Phys.* **2016**, *49*, 243001; c) X. Tu, J. C. Whitehead, T. Nozaki, *Plasma Catalysis. Fundamentals and Applications*, Springer, Cham **2019**; d) A. Bogaerts, X. Tu, J. C. Whitehead, G. Centi, L. Lefferts, O. Guaitella, F. Azzolina-Jury, H.-H. Kim, A. B. Murphy, W. F. Schneider, T. Nozaki, J. C. Hicks, A. Rousseau, F. Thevenet, A. Khacef, M. Carreon, *J. Phys. D Appl. Phys.* **2020**, *53*, 443001; e) A. Bogaerts, E. C. Neyts, O. Guaitella, A. B. Murphy, *Plasma Sources Sci. Technol.* **2022**, *31*, 053002.
- [11] a) Y. Wang, M. Craven, X. Yu, J. Ding, P. Bryant, J. Huang, X. Tu, *ACS Catal.* **2019**, *9*, 10780–10793; b) A. Bogaerts, Q.-Z. Zhang, Y.-R. Zhang, K. Van Laer, W. Wang, *Catal. Today* **2019**, *337*, 3–14; c) N. Wang, H. O. Otor, G. Rivera-Castro, J. C. Hicks, *ACS Catal.* **2024**, *14*, 6749–6798.
- [12] a) M. D. Farahani, Y. Zeng, Y. Zheng, *Energy Sci. Eng.* **2022**, *10*, 1572–1583; b) Z. Ye, L. Zhao, A. Nikiforov, J.-M. Giraudon, Y. Chen, J. Wang, X. Tu, *Adv. Colloid Interface Sci.* **2022**, *308*, 102755.
- [13] a) S. Xu, H. Chen, X. Fan, *Catal. Today* **2023**, *419*, 114144; b) Y. Ma, P. Chen, D. Li, F. Wang, L. Wang, K. Li, P. Ning, X. Wang, K. Ostrikov, *J. Environ. Chem. Eng.* **2024**, *12*, 112383; c) S. Xu, H. Chen, C. Hardacre, X. Fan, *J. Phys. D Appl. Phys.* **2021**, *54*, 233001.
- [14] a) Y.-R. Zhang, K. Van Laer, E. C. Neyts, A. Bogaerts, *Appl. Catal. B* **2016**, *185*, 56–67; b) J. Kruszelnicki, K. W. Engeling, J. E. Foster, M. J. Kushner, *J. Phys. D Appl. Phys.* **2021**, *54*, 104001; c) K. Wu, J. Xiong, Y. Sun, J. Wu, M. Fu, D. Ye, *J. Hazard. Mater.* **2022**, *428*, 128172; d) Y. Xu, N. Liu, Y. Lin,

- X. Mao, H. Zhong, Z. Chang, M. N. Shneider, Y. Ju, *Nat. Commun.* **2024**, *15*, 3092.
- [15] a) C. Ndayirinde, Y. Gorbanev, R.-G. Ciocarlan, R. De Meyer, A. Smets, E. Vlasov, S. Bals, P. Cool, A. Bogaerts, *Catal. Today* **2023**, *419*, 114156; b) C. Yan, C. Waitt, I. Akintola, G. Lee, J. Easa, R. Clarke, F. Geng, D. Poirier, H. O. Otor, G. Rivera-Castro, D. B. Go, C. P. O'Brien, J. C. Hicks, W. F. Schneider, H. Ma, *J. Phys. Chem. C* **2022**, *126*, 9611–9614.
- [16] R. De Meyer, Y. Gorbanev, R.-G. Ciocarlan, P. Cool, S. Bals, A. Bogaerts, *Chem. Eng. J.* **2024**, *488*, 150838.
- [17] a) A. Wang, J. H. Harrhy, S. Meng, P. He, L. Liu, H. Song, *Energy Convers. Manage.* **2019**, *191*, 93–101; b) J. A. Andersen, J. M. Christensen, M. Østberg, A. Bogaerts, A. D. Jensen, *Chem. Eng. J.* **2020**, *397*, 125519; c) J. Sentek, K. Krawczyk, M. Młotek, M. Kalczyńska, T. Kroker, T. Kolb, A. Schenk, K.-H. Gericke, K. Schmidt-Szałowski, *Appl. Catal. B* **2010**, *94*, 19–26; d) L. Wang, Y. Yi, C. Wu, H. Guo, X. Tu, *Angew. Chem. Int. Ed.* **2017**, *56*, 13679–13683.
- [18] a) K. Van Laer, A. Bogaerts, *Plasma Sources Sci. Technol.* **2016**, *25*, 015002; b) K. Van Laer, A. Bogaerts, *Plasma Sources Sci. Technol.* **2017**, *26*, 085007; c) K. Van Laer, A. Bogaerts, *Plasma Processes Polym.* **2017**, *14*, 1600129; d) W. Wang, H.-H. Kim, K. Van Laer, A. Bogaerts, *Chem. Eng. J.* **2018**, *334*, 2467–2479; e) W. S. Kang, H.-H. Kim, Y. Teramoto, A. Ogata, J. Y. Lee, D.-W. Kim, M. Hur, Y.-H. Song, *Plasma Sources Sci. Technol.* **2018**, *27*, 015018; f) J. Kruszelnicki, K. W. Engeling, J. E. Foster, Z. Xiong, M. J. Kushner, *J. Phys. D Appl. Phys.* **2017**, *50*, 025203; g) Z.-u.-I. Mujahid, J. Kruszelnicki, A. Hala, M. J. Kushner, *Chem. Eng. J.* **2020**, *382*, 123038; h) K. Li, X. Lei, H. Cheng, W. Zhang, X. Lu, *Plasma Sources Sci. Technol.* **2024**, *33*, 085013.
- [19] S. Maerivoet, I. Tsonev, J. Slaets, F. Reniers, A. Bogaerts, *Chem. Eng. J.* **2024**, *492*, 152006.
- [20] Y. Wang, Y. Chen, J. Harding, H. He, A. Bogaerts, X. Tu, *Chem. Eng. J.* **2022**, *450*, 137860.
- [21] a) Y. Cai, D. Mei, Y. Chen, A. Bogaerts, X. Tu, *J. Energy Chem.* **2024**, *96*, 153–163; b) J. Li, J. Xu, E. Rebrov, A. Bogaerts, *Chem. Eng. J.* **2024**, submitted.
- [22] Y. Engelmann, P. Mehta, E. C. Neyts, W. F. Schneider, A. Bogaerts, *ACS Sustainable Chem. Eng.* **2020**, *8*, 6043–6054.
- [23] a) B. Loenders, Y. Engelmann, A. Bogaerts, *J. Phys. Chem. C* **2021**, *125*, 2966–2983; b) P.-A. Maitre, M. S. Bieniek, P. N. Kechagiopoulos, *J. Phys. Chem. C* **2022**, *126*, 19987–20003; c) N. Pourali, M. Vasilev, R. Abiev, E. V. Rebrov, *J. Phys. D Appl. Phys.* **2022**, *55*, 395204.
- [24] R. Michiels, Y. Engelmann, A. Bogaerts, *J. Phys. Chem. C* **2020**, *124*, 25859–25872.
- [25] a) P. Mehta, P. Barboun, F. A. Herrera, J. Kim, P. Rumbach, D. B. Go, J. C. Hicks, W. F. Schneider, *Nat. Catal.* **2018**, *1*, 269–275; b) P. Mehta, P. M. Barboun, Y. Engelmann, D. B. Go, A. Bogaerts, W. F. Schneider, J. C. Hicks, *ACS Catal.* **2020**, *10*, 6726–6734; c) Y. Engelmann, K. van't Veer, Y. Gorbanev, E. C. Neyts, W. F. Schneider, A. Bogaerts, *ACS Sustainable Chem. Eng.* **2021**, *9*, 13151–13163.
- [26] Y. Gorbanev, Y. Engelmann, K. van't Veer, E. Vlasov, C. Ndayirinde, Y. Yi, S. Bals, A. Bogaerts, *Catalysts* **2021**, *11*, 1230.
- [27] K. M. Bal, S. Huygh, A. Bogaerts, E. C. Neyts, *Plasma Sources Sci. Technol.* **2018**, *27*, 024001.
- [28] a) A. Jafarzadeh, K. M. Bal, A. Bogaerts, E. C. Neyts, *J. Phys. Chem. C* **2020**, *124*, 6747–6755; b) A. Jafarzadeh, K. M. Bal, A. Bogaerts, E. C. Neyts, *J. Phys. Chem. C* **2019**, *123*, 6516–6525.
- [29] M. Kim, S. Biswas, I. Barraza Alvarez, P. Christopher, B. M. Wong, L. Mangolini, *JACS Au* **2024**, *4*, 2979–2988.
- [30] J. Wang, K. Zhang, M. Mertens, A. Bogaerts, V. Meynen, *Appl. Catal. B* **2023**, *337*, 122977.
- [31] Y. Zhang, H.-Y. Wang, W. Jiang, A. Bogaerts, *New J. Phys.* **2015**, *17*, 083056.
- [32] Q.-Z. Zhang, A. Bogaerts, *Plasma Sources Sci. Technol.* **2018**, *27*, 105013.
- [33] a) Y.-R. Zhang, E. C. Neyts, A. Bogaerts, *J. Phys. Chem. C* **2016**, *120*, 25923–25934; b) Y.-R. Zhang, E. C. Neyts, A. Bogaerts, *Plasma Sources Sci. Technol.* **2018**, *27*, 055008.
- [34] a) Q.-Z. Zhang, A. Bogaerts, *Plasma Sources Sci. Technol.* **2018**, *27*, 035009; b) Q.-Z. Zhang, W.-Z. Wang, A. Bogaerts, *Plasma Sources Sci. Technol.* **2018**, *27*, 065009.
- [35] K. H. R. Rouwenhorst, S. Mani, L. Lefferts, *ACS Sustainable Chem. Eng.* **2022**, *10*, 1994–2000.
- [36] Y. Wang, W. Yang, S. Xu, S. Zhao, G. Chen, A. Weidenkaff, C. Hardacre, X. Fan, J. Huang, X. Tu, *J. Am. Chem. Soc.* **2022**, *144*, 12020–12031.
- [37] R. Snoeckx, R. Aerts, X. Tu, A. Bogaerts, *J. Phys. Chem. C* **2013**, *117*, 4957–4970.
- [38] K. van't Veer, Y. Engelmann, F. Reniers, A. Bogaerts, *J. Phys. Chem. C* **2020**, *124*, 22871–22883.
- [39] a) R. Vertongen, A. Bogaerts, *J. CO<sub>2</sub> Util.* **2023**, *72*, 102510; b) Y. Uytendhouwen, J. Hereijgers, T. Breugelmans, P. Cool, A. Bogaerts, *Chem. Eng. J.* **2021**, *405*, 126618; c) X. Gao, Z. Lin, T. Li, L. Huang, J. Zhang, S. Askari, N. Dewangan, A. Jangam, S. Kawi, *Catalysts* **2021**, *11*, 455.
- [40] A. Unciti-Broceta, E. Rebrov, *Catal. Sci. Technol.* **2024**, *14*, 512–514.
- [41] a) J. Ráhel', D. M. Sherman, *J. Phys. D Appl. Phys.* **2005**, *38*, 547; b) Y. Zhang, J. Li, N. Lu, K. Shang, A. Mizuno, Y. Wu, *Vacuum* **2016**, *123*, 49–53; c) C. Wang, G. Zhang, X. Wang, *Vacuum* **2012**, *86*, 960–964.
- [42] G. De Felice, S. Li, G. Anello, C. Petit, F. Gallucci, E. Rebrov, *Catal. Today* **2024**, *440*, 114832.
- [43] D. Ray, P. M. K. Reddy, C. Subrahmanyam, *Catal. Today* **2018**, *309*, 212–218.
- [44] J. Wang, K. Zhang, S. Kavak, S. Bals, V. Meynen, *Chem. A Eur. J.* **2023**, *29*, e202202670.
- [45] X. Wang, Y. Zhang, W. Luo, A. A. Elzatahy, X. Cheng, A. Alghamdi, A. M. Abdullah, Y. Deng, D. Zhao, *Chem. Mater.* **2016**, *28*, 2356–2362.
- [46] A. Salden, M. Budde, C. A. Garcia-Soto, O. Biondo, J. Barauna, M. Faedda, B. Musig, C. Fromentin, M. Nguyen-Quang, H. Philippot, G. Hasrack, D. Aceto, Y. Cai, F. A. Jury, A. Bogaerts, P. Da Costa, R. Engeln, M. E. Gálvez, T. Gans, T. García, V. Guerra, C. Henriques, M. Motak, M. V. Navarro, V. I. Parvulescu, G. Van Rooij, B. Samojedan, A. Sobota, P. Tosi, X. Tu, O. Guaitella, *J. Energy Chem.* **2023**, *86*, 318–342.
- [47] G. De Felice, S. Li, Y. Chung, J. Canals Busqueta, Z. Ma, F. Gallucci, E. Rebrov, *Chem. Eng. Sci.* **2025**, *302*, 120805.
- [48] a) M. J. Kirkpatrick, W. C. Finney, B. R. Locke, *Catal. Today* **2004**, *89*, 117–126; b) N. Peters, L. Schücke, K. Ollegott, C. Oberste-Beulmann, P. Awakowicz, M. Muhler, *Plasma Processes Polym.* **2021**, *18*, 2000127.
- [49] J. W. Gregory, N. Pourali, Y. Gong, R. I. Walton, V. Hessel, E. V. Rebrov, *Appl. Catal. A* **2024**, *675*, 119639.
- [50] S. D. Svetlov, D. A. Sladkovskiy, K. V. Semikin, A. V. Utemov, R. S. Abiev, E. V. Rebrov, *Catalysts* **2021**, *11*, 1538.
- [51] D. Khunda, S. Li, N. Cherkasov, M. Z. M. Rishard, A. L. Chaffee, E. V. Rebrov, *React. Chem. Eng.* **2023**, *8*, 2223–2233.
- [52] N. García-Moncada, G. van Rooij, T. Cents, L. Lefferts, *Catal. Today* **2021**, *369*, 210–220.
- [53] a) X. Chen, Z. Sheng, S. Murata, S. Zen, H.-H. Kim, T. Nozaki, *J. CO<sub>2</sub> Util.* **2021**, *54*, 101771; b) N. Bouchoul, H. Touati, E. Fourré, J.-M. Clacens, C. Batiot-Dupeyrat, *Fuel* **2021**, *288*, 119575.
- [54] H. Lee, H. Sekiguchi, *J. Phys. D Appl. Phys.* **2011**, *44*, 274008.
- [55] J. Martin-del-Campo, M. Uceda, S. Coulombe, J. Kopyscinski, *J. CO<sub>2</sub> Util.* **2021**, *46*, 101474.
- [56] Q. F. Lin, Y. M. Jiang, C. Z. Liu, L. W. Chen, W. J. Zhang, J. Ding, J. G. Li, *Energy Rep.* **2021**, *7*, 4064–4070.
- [57] A. S. Issangya, R. A. Cocco, S. B. Reddy Karri, T. M. Knowlton, J. Wei Chew, *Chem. Eng. Sci.* **2022**, *260*, 117837.
- [58] a) J. Zhou, T. Wei, X. An, *Phys. Chem. Chem. Phys.* **2023**, *25*, 1538–1545; b) A. Pandiyan, V. Kyriakou, D. Neagu, S. Welzel, A. Goede, M. C. M. van de Sanden, M. N. Tsampas, *J. CO<sub>2</sub> Util.* **2022**, *57*, 101904; c) P. J. Bruggeman, R. R. Frontiera, U. R. Kortshagen, M. J. Kushner, S. Lincic, G. C. Schatz, H. Andaraarachchi, S. Exarhos, L. O. Jones, C. M. Mueller, C. C. Rich, C. Xu, Y. Yue, Y. Zhang, *J. Appl. Phys.* **2021**, *129*, 200902; d) J. Osorio-Tejada, M. Escriba-Gelonch, R. Vertongen, A. Bogaerts, V. Hessel, *Energy Environ. Sci.* **2024**, *17*, 5833–5853; e) J. Sun, R. Zhou, J. Hong, Y. Gao, Z. Qu, Z. Liu, D. Liu, T. Zhang, R. Zhou, K. Ostrikov, P. Cullen, E. C. Lovell, R. Amal, A. R. Jalili, *Appl. Catal. B* **2024**, *342*, 123426; f) S. Jia, X. Tan, L. Wu, X. Ma, L. Zhang, J. Feng, L. Xu, X. Song, Q. Zhu, X. Kang, X. Sun, B. Han, *Chem. Sci.* **2023**, *14*, 13198–13204.
- [59] a) C. Ampelli, F. Tavella, D. Giusi, A. M. Ronsisvalle, S. Perathoner, G. Centi, *Catal. Today* **2023**, *421*, 114217; b) D. Giusi, C. Ampelli, C. Genovese, S. Perathoner, G. Centi, *Chem. Eng. J.* **2021**, *408*, 127250; c) D. Giusi, M. Miceli, C. Genovese, G. Centi, S. Perathoner, C. Ampelli, *Appl. Catal. B* **2022**, *318*, 121845; d) V. Longo, L. De Pasquale, F. Tavella, M. Barawi, M. Gomez-Mendoza, V. de la Peña O'Shea, C. Ampelli, S. Perathoner, G. Centi, C. Genovese, *EES Catal.* **2024**, *2*, 1164–1175.
- [60] a) P. Rumbach, D. M. Bartels, R. M. Sankaran, D. B. Go, *Nat. Commun.* **2015**, *6*, 7248; b) R. Gopalakrishnan, E. Kawamura, A. J. Lichtenberg, M. A. Lieberman, D. B. Graves, *J. Phys. D Appl. Phys.* **2016**, *49*, 295205.

- [61] a) L. Di, J. Zhang, X. Zhang, H. Wang, H. Li, Y. Li, D. Bu, *J. Phys. D Appl. Phys.* **2021**, *54*, 333001; b) M. Boutonnet Kizling, S. G. Järås, *Appl. Catal. A* **1996**, *147*, 1–21; c) P. Mierczynski, A. Mierczynska-Vasilev, M. Szyrkowska-Jozwik, K. Vasilev, *Catal. Commun.* **2024**, *187*, 106839.
- [62] J. Sun, D. Alam, R. Daiyan, H. Masood, T. Zhang, R. Zhou, P. J. Cullen, E. C. Lovell, A. Jalili, R. Amal, *Energy Environ. Sci.* **2021**, *14*, 865–872.
- [63] S. Meng, A. Wang, P. He, H. Song, *J. Phys. Chem. Lett.* **2020**, *11*, 3877–3881.
- [64] D. Mei, X. Zhu, C. Wu, B. Ashford, P. T. Williams, X. Tu, *Appl. Catal. B* **2016**, *182*, 525–532.
- [65] X. Chen, Y. Li, X. Pan, D. Cortie, X. Huang, Z. Yi, *Nat. Commun.* **2016**, *7*, 12273.
- [66] W. A. Saoud, N. Belkessa, A. A. Azzaz, V. Rochas, V. Mezino, M.-A. Passet, S. Lechevin, A. Genouel, S. Rouxel, D. Monsimert, A. Bouzaza, A. Gloux, D. Cantin, A. A. Assadi, *Chem. Eng. J.* **2023**, *468*, 143710.
- [67] A. A. Assadi, A. Bouzaza, C. Vallet, D. Wolbert, *Chem. Eng. J.* **2014**, *254*, 124–132.
- [68] W.-C. Chung, I. Y. Tsao, M.-B. Chang, *Energy Convers. Manage.* **2018**, *164*, 417–428.
- [69] L. R. Winter, J. G. Chen, *Joule* **2021**, *5*, 300–315.
- [70] S. Kumari, S. Pishgar, M. E. Schwarting, W. F. Paxton, J. M. Spurgeon, *Chem. Commun.* **2018**, *54*, 13347–13350.
- [71] S. Lin, X. Zhang, L. Chen, Q. Zhang, L. Ma, J. Liu, *Green Chem.* **2022**, *24*, 9003–9026.
- [72] P. Peng, P. Chen, M. Addy, Y. Cheng, Y. Zhang, E. Anderson, N. Zhou, C. Schiappacasse, R. Hatzenbeller, L. Fan, S. Liu, D. Chen, J. Liu, Y. Liu, R. Ruan, *Chem. Commun.* **2018**, *54*, 2886–2889.
- [73] R. Hawtof, S. Ghosh, E. Guarr, C. Xu, R. Mohan Sankaran, J. N. Renner, *Sci. Adv.* **5**, eaat5778.
- [74] J. R. Christianson, D. Zhu, R. J. Hamers, J. R. Schmidt, *J. Phys. Chem. B* **2014**, *118*, 195–203.
- [75] a) S. Schüttler, A. L. Schöne, E. Jeß, A. R. Gibson, J. Golda, *Phys. Chem. Chem. Phys.* **2024**, *26*, 8255–8272; b) J. Liu, B. He, Q. Chen, J. Li, Q. Xiong, G. Yue, X. Zhang, S. Yang, H. Liu, Q. H. Liu, *Sci. Rep.* **2016**, *6*, 38454; c) R. Zhou, T. Zhang, R. Zhou, S. Wang, D. Mei, A. Mai-Prochnow, J. Weerasinghe, Z. Fang, K. Ostrikov, P. J. Cullen, *Green Chem.* **2021**, *23*, 2977–2985; d) S. Liang, Q. Wu, C. Wang, R. Wang, D. Li, Y. Xing, D. Jin, H. Ma, Y. Liu, P. Zhang, X. Zhang, *Proc. Natl. Acad. Sci. USA* **2024**, *121*, e2410504121.
- [76] D. Gao, I. Zegkinoglou, N. J. Divins, F. Scholten, I. Sinev, P. Grosse, B. Roldan Cuenya, *ACS Nano* **2017**, *11*, 4825–4831.
- [77] a) L. Xu, Q. Jiang, Z. Xiao, X. Li, J. Huo, S. Wang, L. Dai, *Angew. Chem. Int. Ed.* **2016**, *55*, 5277–5281; b) Y. Wang, Y. Zhang, Z. Liu, C. Xie, S. Feng, D. Liu, M. Shao, S. Wang, *Angew. Chem. Int. Ed.* **2017**, *56*, 5867–5871; c) L. Tao, C.-Y. Lin, S. Dou, S. Feng, D. Chen, D. Liu, J. Huo, Z. Xia, S. Wang, *Nano Energy* **2017**, *41*, 417–425.
- [78] S. Bepalko, J. Mizeraczyk, *Energies* **2022**, *15*, 9431.
- [79] J. Mizeraczyk, M. Jasiński, *Eur. Phys. J. Appl. Phys.* **2016**, *75*, 24702.
- [80] D. H. Lee, H. Kang, Y. Kim, H. Song, H. Lee, J. Choi, K.-T. Kim, Y.-H. Song, *Fuel Process. Technol.* **2023**, *247*, 107761.
- [81] M. Okubo, *Plasma Chem. Plasma Process.* **2022**, *42*, 3–33.
- [82] I. Stasiulaitiene, D. Martuzevicius, V. Abromaitis, M. Tichonovas, J. Baltrusaitis, R. Brandenburg, A. Pawelec, A. Schwöck, *J. Cleaner Prod.* **2016**, *112*, 1804–1812.
- [83] H. Radhakrishnan, S. Gnangbe, A. Duereh, S. U. Iffat Uday, A. Lusi, H. Hu, H. Hu, M. M. Wright, X. Bai, *Green Chem.* **2024**, *26*, 9156–9175.
- [84] J. O. Pou, E. Estopañán, J. Fernandez-Garcia, R. Gonzalez-Olmos, *Processes* **2022**, *10*, 1851.
- [85] A. Anastasopoulou, S. Butala, J. Lang, V. Hessel, Q. Wang, *Ind. Eng. Chem. Res.* **2016**, *55*, 8141–8153.
- [86] J. L. Osorio-Tejada, E. Rebrov, V. Hessel, *Int. J. Life Cycle Assess.* **2023**, *28*, 1590–1603.
- [87] N. S. Matin, W. P. Flanagan, *Int. J. Hydrogen Energy* **2024**, *49*, 1405–1413.
- [88] A. Ramos, A. Rouboa, *Renew. Sustain. Energy Rev.* **2022**, *153*, 111762.
- [89] I. Tsonev, H. Ahmadi Eshtehardi, M.-P. Delplancke, A. Bogaerts, *Sustain. Energy Fuels* **2024**, *8*, 2191–2209.
- [90] E. Delikonstantis, E. Igos, M. Augustinus, E. Benetto, G. D. Stefanidis, *Sustain. Energy Fuels* **2020**, *4*, 1351–1362.
- [91] C. O'Modhrain, G. Trenchev, Y. Gorbanev, A. Bogaerts, *ACS Eng. Au.* **2024**, *4*, 333–344.
- [92] R. Schenk, V. Hessel, C. Hofmann, J. Kiss, H. Löwe, A. Ziogas, *Chem. Eng. J.* **2004**, *101*, 421–429.
- [93] A. Yamamoto, S. Mori, M. Suzuki, *Thin Solid Films* **2007**, *515*, 4296–4300.
- [94] R. Burlica, D.-E. Cretu, O. Beniuga, D. Astanei, *Appl. Sci.* **2022**, *12*, 10403.
- [95] M. A. Malik, S. Xiao, K. H. Schoenbach, *J. Hazard. Mater.* **2012**, *209–210*, 293–298.
- [96] M. Radoiu, A. Mello, *Plasma Process. Polym.* **2024**, *21*, 2300200.

Manuscript received: November 25, 2024

Revised manuscript received: January 19, 2025

Accepted manuscript online: January 29, 2025

Version of record online: February 23, 2025